



Constraining the timing and processes of pediment formation and dissection: implications for long-term evolution in the Western Cape, South Africa

Janet C. Richardson¹, Veerle Vanacker², David M. Hodgson³, Marcus Christl⁴, and Andreas Lang⁵

¹Geography and Geology: Department of History, Geography and Social Sciences,
Edge Hill University, Ormskirk, L39 4QP, UK

²Earth and Life Institute, Centre for Earth and Climate Research, Université catholique de Louvain,
Louvain-la-Neuve, 1348, Belgium

³School of Earth and Environment, University of Leeds, Leeds, LS2 9JT, UK

⁴Ion Beam Physics, ETH Zürich, Otto-Stern-Weg 5, 8093 Zurich, Switzerland

⁵Department of Geography and Geology, Universität Salzburg, 5020 Salzburg, Austria

Correspondence: Janet C. Richardson (janet.richardson@edgehill.ac.uk)

Received: 13 August 2024 – Discussion started: 18 September 2024

Revised: 15 January 2025 – Accepted: 12 February 2025 – Published: 29 April 2025

Abstract. Pediment surfaces are a widespread feature of the southern African landscape and have long been regarded as ancient landforms. Cosmogenic nuclide data from four pediment surfaces in the Gouritz catchment, Western Cape, South Africa, are reported, including boulder surface samples and a depth profile through a colluvial pediment deposit. Pediment surfaces are remarkably stable with long-term denudation rates between 0.3 and 1.0 m Myr⁻¹, and their ¹⁰Be concentrations approach or are at secular equilibrium. Duricrusts have developed in the pediments and are preserved in some locations, which represent an internal geomorphic threshold limiting denudation and indicate at least 2 Myr of geomorphic stability following pediment formation. The pediments and the neighbouring Cape Fold Belt are deeply dissected by small-order streams that form up to 280 m deep river valleys in the resistant fold belt bedrock geology, indicating a secondary incision phase of the pediments by these smaller-order streams. Using the broader stratigraphic and geomorphic framework, the minimum age of pediment formation is considered to be Miocene. Several pediment surfaces grade above the present trunk valleys of the Gouritz River, which suggests that the trunk rivers are long-lived features that acted as local base levels during pediment formation and later incised pediments to present levels. The geomorphic processes controlling the formation and evolution of the pediments varied over time, with pediments formed by hillslope diffusive processes as shown by the lack of fluvial indicators in the colluvial deposits and later development by fluvial processes with small tributaries dissecting the pediments. Integrating various strands of evidence indicates that the pediments are long-lived features.

1 Introduction

Recent advancements in geochronology allow erosion rates and exposure ages of landforms to be established and more precise constraints to be placed on landscape evolution. Establishing erosion rates and landform ages is essential for linking the evolution of drainage systems to downstream aggradation processes (e.g. Gallagher and Brown, 1999;

Chappell et al., 2006; Tinker et al., 2008a; Wittmann et al., 2009; Sømme et al., 2011; Romans et al., 2016), constraining surface uplift and tectonic processes (e.g. Brook et al., 1995; Burbank et al., 1996; Granger et al., 1997; Jackson et al., 2002; Wittmann et al., 2007; Bellin et al., 2014; Vanacker et al., 2015), and palaeo-climate reconstructions (e.g. Margerison et al., 2005; Dunai et al., 2005; Owen et al., 2005; Willenbring and von Blackenburg, 2010). Reconstructing ancient

landforms and landscape development is challenging due to fragmented preservation and increasing signal overprinting forming a landscape palimpsest (e.g. Chorley et al., 1984; Bloom, 2002; Bishop, 2007; Jerolmack and Paola, 2010; Richardson et al., 2016). However, ancient landscapes and landforms cover a large portion of the globe (e.g. (1) Australia – e.g. Ollier, 1991; Ollier and Pain, 2000; Twidale, 2007a, b; (2) southern South Africa – e.g. Du Toit, 1954; King, 1956a; (3) South America – e.g. King, 1956b; Carignano et al., 1999; Demoulin et al., 2005; Panario et al., 2014; Peulvast and Bétard, 2015; (4) Asia – e.g. Gorelov et al., 1970; Gunnell et al., 2007; Vanacker et al., 2007; and (5) Europe – e.g. Lidmar-Bergström, 1988; Bessin et al., 2015) and offer important insights into long-term Earth surface dynamics and landscape evolution (indicating variation in erosion and deposition). Further, pediments and planation surfaces can offer insights into mantle dynamics as they are characterised by undulations with middle (several tens of kilometres) to very long wavelengths (several thousands of kilometres) characteristic of lithospheric and mantle deformations (e.g. Braun et al., 2014; Guillocheau et al., 2018).

The formation of pediments is contentious and four categories of landscape evolution models (Fig. 1) exist that address the evolution of pediments and surrounding mountain belts (Dohrenward and Parsons, 2009): (1) range front retreat where channelised fluvial processes are dominant (e.g. Gilbert, 1877; Paige, 1912; Howard, 1942); (2) range front retreat where diffuse hillslope and piedmont processes are dominant (e.g. Lawson, 1915; Rich, 1935; Kesel, 1977; Bourne and Twidale, 1998; Dauteuil et al., 2015); (3) range front retreat as a result of fluvial and diffusive erosion processes (e.g. Bryan, 1923; Sharp, 1940); and (4) lowering of the range due to channelised flow, catchment development and fluvial incision (e.g. Lustig, 1969; Parsons and Abrahams, 1984). Model type 1 also acknowledges the occurrence of diffusive processes and model type 2 the occurrence of channelised erosion processes but consider them as subsidiary formation processes (Gilbert, 1877; Rich, 1935; Howard, 1942). Model type 3 integrates fluvial and diffusive erosion processes, and their relative importance depends on the geomorphic setting (Bryan, 1923; Sharp, 1940) with a dominance of diffusive processes in regions with erosion-resistant bedrock lithologies, ephemeral streams and low range. Model type 4 is associated with drainage basin development in the range and does not require parallel retreat of the mountain front to form the pediment surfaces (Lustig, 1969; Parsons and Abrahams, 1984).

The geomorphology of southern Africa has long intrigued earth scientists (Rogers, 1903; Davis, 1906; Dixey, 1944; King, 1948, 1949, 1953). Fundamental questions related to long-term landscape development remain contentious, such as the mechanisms and timing of surface uplift (e.g. Gallagher and Brown, 1999; Brown et al., 2002; Tinker et al., 2008b; Kounov et al., 2009; Decker et al., 2013; Wildman et al., 2015, 2017; Stanley et al., 2021) and the chronolog-

ical framework of the main phases of landscape development (Du Toit, 1937, 1954; King, 1951; Burke, 1996; Partridge, 1998; Brown et al., 2002; Doucouré and de Wit, 2003; de Wit, 2007; Kounov et al., 2015). Cosmogenic nuclides (CRNs) produced in situ can offer key information to unravel questions related to landscape development and evolution and have been applied to ancient landforms within southern Africa (Fleming et al., 1999; Cockburn et al., 2000; Bierman and Caffee, 2001; van der Wateren and Dunai, 2001; Kounov et al., 2007; Codilean et al., 2008; Dirks et al., 2010; Decker et al., 2011; Erlanger et al., 2012; Chadwick et al., 2013; Decker et al., 2013). However, studies based on CRNs produced in situ in the region south of the Great Escarpment are sparse (e.g. Scharf et al., 2013; Bierman et al., 2014; Kounov et al., 2015).

Pediments or erosional surfaces have been investigated in South Africa since the 1950s (King, 1953, 1963; Partridge and Maud, 1987) and have denudation rates that are an order of magnitude lower than those in other landforms within southern Africa (van der Wateren and Dunai, 2001; Bierman et al., 2014; Kounov et al., 2015; Fig. 2). The pediment surfaces were inferred as being Early Cenozoic to Jurassic in age by King (1963). Large-scale erosional features are also a feature of the wider African continent, and extensive research has been undertaken to understand mantle dynamics associated with plateau formation (e.g. Braun et al., 2014; Dauteuil et al., 2015; Guillocheau et al., 2015, 2018). In this paper, we present new isotopic data from pediment landforms in southern South Africa. The main aim of the paper is to constrain landscape development using ^{10}Be isotopes produced in situ and to establish denudation rates and landform exposure ages. The objectives of the paper are to (1) assess the formative process associated with pediment evolution, (2) assess the cosmogenic data within a wider geomorphic and geologic framework in order to test the performance of cosmogenic dating in a geomorphic setting with very low denudation rates, and (3) discuss the implications for the wider landscape development of southern South Africa.

2 Regional setting

2.1 Geological setting

In the Western Cape, South Africa, the geology is dominated by strata of the Cape (Early Ordovician to Early Carboniferous) and Karoo supergroups (Late Carboniferous to Early Jurassic) (Johnson et al., 1995; Frimmel et al., 2001) (Fig. 2), which are composed of various sandstone, siltstone and mudstone successions. Both supergroups have been subject to low-grade burial metamorphism (Frimmel et al., 2001), with localised contact metamorphism during Jurassic dolerite intrusion (Johnson et al. 1995) and an estimated 6–7 km of exhumation during the Early Cretaceous (Tinker et al., 2008a; Wildman et al., 2015). Tectonic shortening during the latest Palaeozoic to Early Mesozoic of the

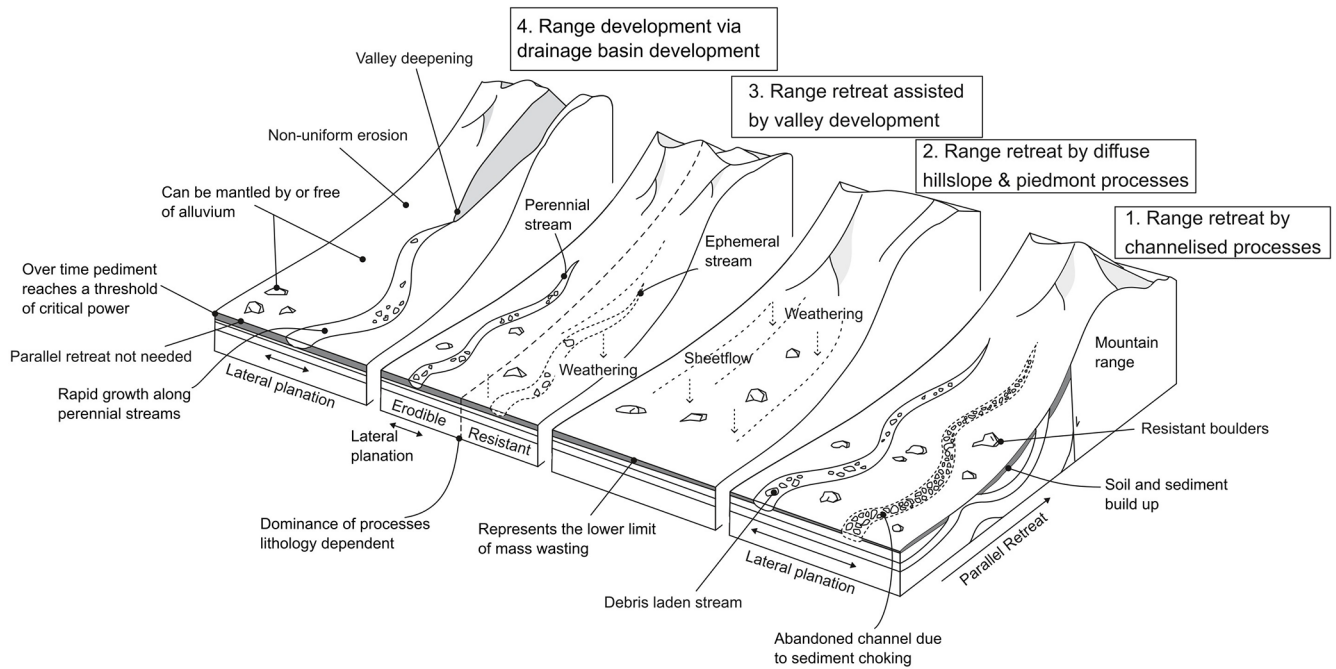


Figure 1. Pediment evolution models showing the range of processes that can shape pediments: (1) range retreat by channelised processes adapted from Gilbert (1877), Paige (1912) and Howard (1942); (2) range retreat by diffuse hillslope and piedmont processes adapted from Lawson (1915), Rich (1935), Kesel (1977), Bourne and Twidale (1998), and Dauteuil et al. (2015); (3) range retreat assisted by valley development adapted from Bryan (1923) and Sharp (1940); and (4) range development via drainage basin development adapted from Lustig (1969) and Parsons and Abrahams (1984).

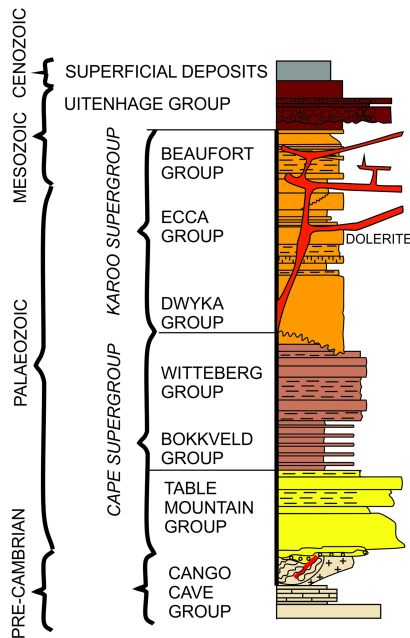


Figure 2. Stratigraphic chart showing the major lithostratigraphic units of the Western Cape, South Africa.

Cape and Karoo supergroups (Tankard et al., 2009; Hansma et al., 2016) have resulted in east–west-trending, northward-

verging and eastward-plunging folds that decrease in amplitude and shorten northwards and form the backbone of the exhumed Cape Fold Belt (CFB) (Paton, 2006; Tinker et al., 2008b; Scharf et al., 2013; Spikings et al., 2015). During the Mesozoic, the rifting of Gondwana initiated large-scale denudation across southern Africa. Using apatite fission track analyses of outcrop and borehole samples, Tinker et al. (2008a) concluded that the southern Cape escarpment and coastal plain have underwent 3.3 to 4.5 km of denudation since the Middle–Late Cretaceous and potentially 1.5 to 4 km within the Early Cretaceous, using a thermal gradient of $\sim 20\text{ }^{\circ}\text{C km}^{-1}$. Wildman et al. (2015) processed 75 apatite fission track and 8 zircon fission track data from outcrop and boreholes across the southwestern cape of South Africa (from coast to the escarpment). Using a thermal model and a geothermal gradient of $22\text{ }^{\circ}\text{C km}^{-1}$, they obtained an average of 4.5 km denudation in the Mesozoic, from the Late Jurassic to the Early Cretaceous. However, their estimates range between 2.2 and 8.8 km of denudation using the upper and lower ranges of the geothermal gradient and possible thermal histories bounded by 95 % significance intervals, which provides uncertainty on the inferred exhumation model. Richardson et al. (2017) used reconstructed geological cross sections, tied to apatite fission track data, and drainage reconstruction to model up to 4–11 km of denudation across the Western Cape, with significant exhumation in

the Early Cretaceous and lower amounts in the Late Cretaceous.

The mechanisms of regional uplift during the Mesozoic, related to the anomalous height of southern Africa, are contentious, with landscape evolution associated with either mantle plumes (Nyblade and Robinson, 1994; Ebinger and Sleep, 1998) or plate tectonics, with uplift along flexures (Moore et al., 2009) resulting in epeirogenic uplift (Brown et al., 1990). Furthermore, the occurrence and timing of later Cenozoic uplift is disputed (e.g. Brown et al., 2002; van der Beek et al., 2002). Burke (1996) proposed that the most recent uplift phase occurred at ~ 30 Ma due to a thermal anomaly, and Green et al. (2016) also argued for Cenozoic uplift within southern South Africa that caused the localised incision of the Gouritz River into the Swartberg mountain range. Partridge and Maud (1987) argued for two phases of uplift during the Neogene, with a phase around 18 Ma and a more recent phase at 2.58 Ma. Brown et al. (2002) and van der Beek et al. (2002) have questioned Cenozoic uplift based on apatite fission track thermochronology, which does not have a signal for recent uplift.

Figure 3 provides an overview of published geochronological studies in southern South Africa that used either apatite (U–Th)/He and apatite fission track analysis to document landscape denudation from the Cretaceous to the modern day or cosmogenic radionuclides produced in situ (^{26}Al , ^{10}Be , ^3He , ^{21}Ne) to date landforms. Apatite (U–Th)/He and fission track data (Fig. 3) indicate high rates of denudation (up to 175 m Myr^{-1} ; Tinker et al., 2008b) with respect to the present-day rates towards the end of the Lower Cretaceous (100–80 Ma) that decreased to up to 95 m Myr^{-1} by the Late Cretaceous (90–70 Ma; Brown et al., 2002). Flowers and Schoene (2010) report negligible erosion since the Cretaceous, with rates as low as 5 m Myr^{-1} by the Late Eocene (36 Myr; Cockburn et al., 2000). Cosmogenic studies support low erosion rates within southern South Africa since the start of the Cenozoic (Fig. 3; Fleming et al., 1999; Cockburn et al., 2000; Bierman and Caffee, 2001; van der Wateren and Dunai, 2001; Kounov et al., 2007; Codilean et al., 2008; Dirks et al., 2010; Decker et al., 2011; Erlanger et al., 2012; Chadwick et al., 2013; Decker et al., 2013; Scharf et al., 2013; Bierman et al., 2014; Kounov et al., 2015). The majority of landforms are eroding very slowly, with mean denudation rates ranging between 9.4 m Myr^{-1} for the escarpment faces to 0.85 m Myr^{-1} for pediments (Fig. 3), although 62 m Myr^{-1} has been measured for one escarpment face retreat (Fleming et al., 1999). In contrast, the Great Escarpment in the South African interior has higher fluvial incision rates than southern South Africa: cosmogenic ^3He channel bed denudation rates range between 14 and 255 m Myr^{-1} and valley side and valley top denudation rates range between 11 and 50 m Myr^{-1} for the Klip and Mooi rivers and Schoonspruit, tributaries of the Orange River (Keen-Zebert et al., 2016).

Southern South Africa, below the Great Escarpment, is currently tectonically quiescent with only minor Quaternary-

active faults (Bierman et al., 2014) and low denudation and sediment production rates (Kounov et al., 2007; Scharf et al., 2013). Minimum exposure ages for pediments range from 0.29 ± 0.02 Ma (Bierman et al., 2014) to 5.18 ± 0.18 Ma (van der Wateren and Dunai, 2001) with a mean minimum exposure age of 1.87 Ma (Pleistocene; van der Wateren and Dunai, 2001; Bierman et al., 2014; Kounov et al., 2015).

The climate of southern South Africa has gradually moved towards more arid conditions since the Cretaceous (Partridge, 1997; van Niekerk et al., 1999) with an abrupt change from humid/tropical to arid conditions at the end of the Cretaceous (Partridge and Maud, 2000) as shown by silcrete formation and saline soils (Partridge and Maud, 1987). Although there is general agreement about the overall aridification trend since the Cretaceous, several authors have argued that wetter phases occurred from 65–30 Ma (Burke, 1996) or that the arid phase started as late as 18 Ma (Partridge and Maud, 1987). The present-day climate of the Western Cape is primarily semi-arid (Dean et al., 1995), while the coastal region has a Mediterranean type climate (Midgley et al., 2003).

2.2 Sample sites

The sampling sites are located within the large antecedent Gouritz catchment (Fig. 4), where morphometric analysis has identified the presence of flat surfaces or pediments that carry a thin sedimentary cover (< 1 m), hereafter called alluviated pediments (Richardson et al., 2016). The alluviated pediments grade away from the Cape Fold Belt (CFB) into adjacent alluvial plains, and samples were collected from pediments on the northern flank of the Swartberg and Witteberg mountains (CFB) around Laingsburg, Floriskraal, Leeuwgat and Prince Albert (Fig. 4a). Samples were taken from five deeply dissected alluviated pediments ranging in surface area between < 1 and 20 km^2 and displaying slope angles below 10° , with most of the slopes below 4° (Fig. 5).

The alluviated pediments are composed of unconsolidated, poorly sorted gravel to boulder material in a matrix of sand (Fig. 6) that unconformably overlies folded rocks of the Karoo Supergroup (Fig. 3b). Some pediments are capped by silcrete, calcrete or ferricrete (Helgren and Butzer, 1977; Summerfield, 1983; Marker and Holmes, 1999; Partridge, 1999; Partridge and Maud, 2000; Marker et al., 2002). Ferricrete is dominant on the Laingsburg pediment. The silcrete is assigned to the Grahamstown Formation (Fig. 4b) that has poor age control (Mountain, 1980; Summerfield, 1983) due to the lack of formal identification of the extent of the silcretes. Electron spin resonance ages for two silcrete caps in the Kleine Karoo were dated at 7.3 and 9.4 Ma (Hagedorn, 1988).

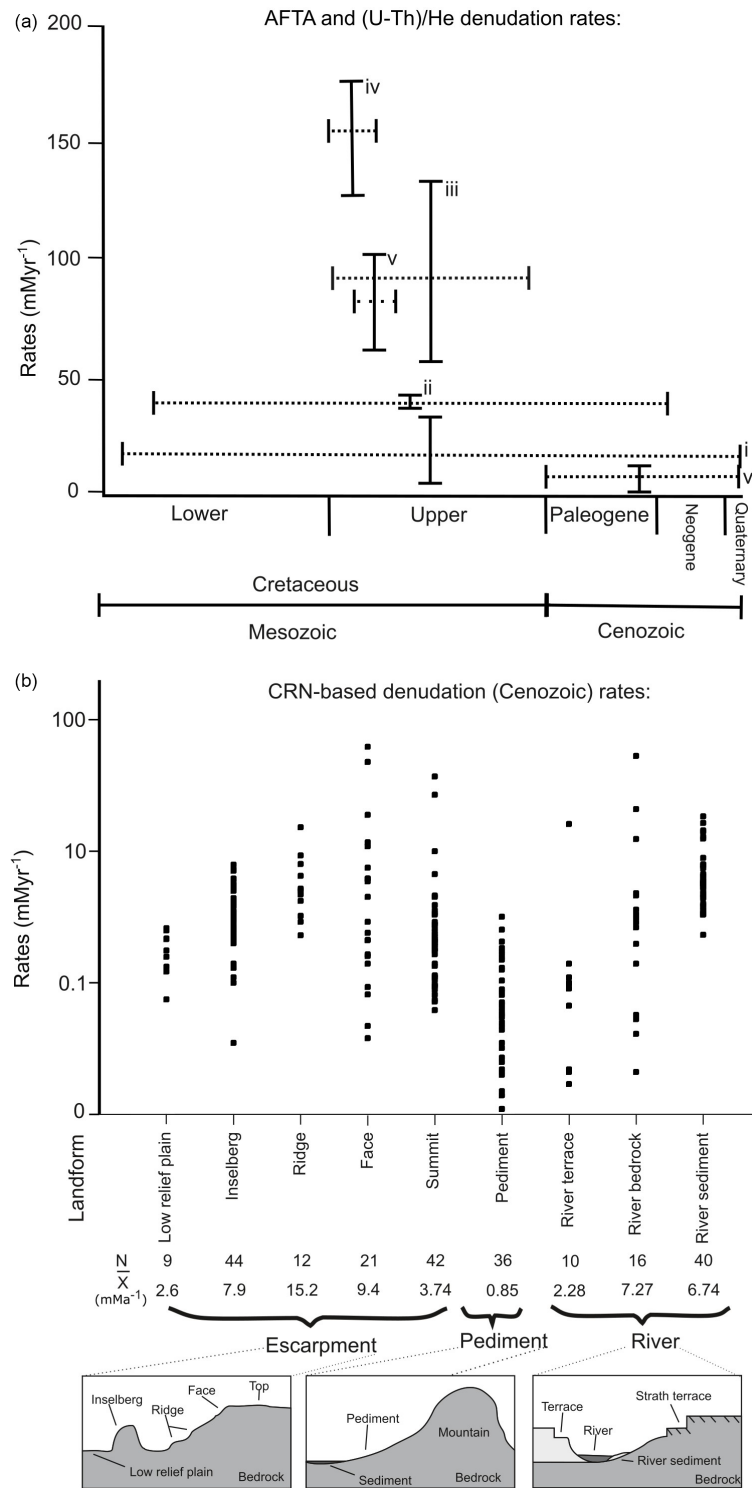


Figure 3. Published exhumation and denudation rates for southern Africa. **(a)** Apatite fission track and (U–Th) / He data show large variation in exhumation rates since the Cretaceous, and error bars show the range in exhumation rates and integration time frame and include data from Gallagher and Brown (1999) (i), Cockburn et al. (2000) (ii), Brown et al. (2002) (iii), Tinker et al. (2008b) (iv), Kounov et al. (2009) (v), and Flowers and Schoene (2010) (vi). **(b)** In situ cosmogenic-nuclide-derived (¹⁰Be, ²⁶Al, ²¹Ne and ³He) denudation rates for escarpment, pediment and fluvial landforms. Cosmogenic data are from the following sources: Fleming et al. (1999), Cockburn et al. (2000), Bierman and Caffee (2001), van der Wateren and Dunai (2001), Kounov et al. (2007), Codilean et al. (2008), Dirks et al. (2010), Decker et al. (2011), Erlanger et al. (2012), Chadwick et al. (2013), Decker et al. (2013), Scharf et al. (2013), Bierman et al. (2014), and Kounov et al. (2015).

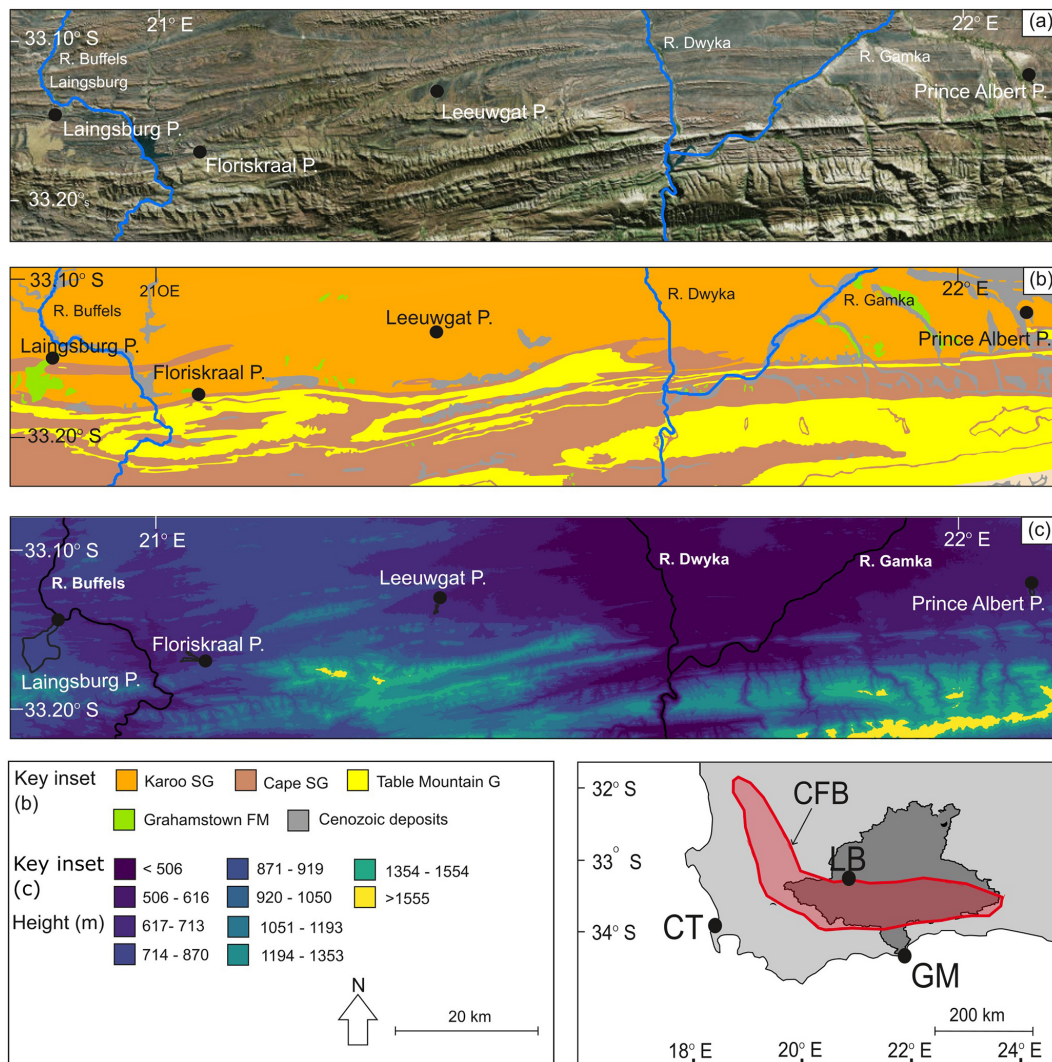


Figure 4. (a) Pediment locations, the inset showing the location of the Gouritz catchment within South Africa, where CT is Cape Town, LB is Laingsburg, GM is Gouritzmond and the red polygon is the location of the Cape Fold Belt (CFB); (b) underlying geology below the pediments; and (c) pediment elevations (in m.a.s.l.) as shown by elevation bins categorised by natural breaks in the elevation data. Aerial imagery for (a) is from ESRI, and geology information for (b) was provided by the Geology Society of South Africa.

3 Methodology

3.1 Cosmogenic radionuclide (CRN) dating

Two types of samples were collected for CRN analyses in 2014: five rock samples from alluviated pediment surfaces and clasts from one depth profile in the Laingsburg pediment (Fig. 7, Table 1). Quartzite boulders from the Table Mountain Group (Cape Supergroup) that were sampled at the surface of the pediments have a > 1 m diameter along their longest axis. For the depth profile in the pediment, quartzite clasts (> 25 cm diameter) were taken at the following depths (cm) below ground level: 0, 30, 85, 150 and 255 (Table 1).

The samples were processed for in situ cosmogenic ^{10}Be following standard methods as described in von Blancken-

burg et al. (2004) and Vanacker et al. (2007). Rock samples were crushed and sieved, and rock fragments of 250 to 500 μm diameter were selected for further lab processing. Quartz minerals were extracted by chemical leaching with a low concentration of acids (HCl , HNO_3 and HF) in an overhead shaker. Purified quartz samples were then leached with 24 % HF for 1 h to remove meteoric ^{10}Be , followed by spiking the sample with 150 μg of ^9Be and total decomposition in concentrated HF . The beryllium in solution was extracted by ion exchange chromatography as described in von Blanckenburg et al. (1996). The $^{10}\text{Be}/^9\text{Be}$ ratios were measured using an accelerator mass spectrometer (AMS) at the 500 kV Tandy facility at ETH Zürich (Christl et al., 2013). Measured $^{10}\text{Be}/^9\text{Be}$ ratios were normalised to the ETH in-house secondary standard S2007N with a

Table 1. Site-specific information of the sampling sites for cosmogenic radionuclide analysis. All samples are taken from quartzite boulders that were sampled either on the surface of the pediment (sample type is surf) or at depth (sample type is depth). The density of the sample or overburden (for depth samples) has been determined based on published density data of quartzite boulders and depth profiles in pediments by, respectively, Scharf et al. (2013) and Kounov et al. (2015). Cover correction has been applied to depth profile samples; for surface samples this is not applicable (n/a).

Sample ID	Sample type	Name	Latitude (° S)	Longitude (° E)	Elevation (m)	Density (g cm ⁻³)	Topographic shielding	Cover correction
SA-PA_ped	Surf	Prince Albert	33.203	22.082	703	2.7	1.00	n/a
SA-LB_ped1	Surf	Laingsburg	33.246	20.872	764	2.7	1.00	n/a
SA-LB_ped2	Surf	Floriskraal	33.285	21.050	706	2.7	1.00	n/a
SA-LB_ped3	Surf	Leeuwgat	33.221	21.347	691	2.7	1.00	n/a
SA-LB_ped4	Surf	Laingsburg	33.261	20.854	791	2.7	1.00	n/a
SA-LB_DP0	Depth	Laingsburg	33.256	20.851	776	1.6	0.99	n/a
SA-LB_DP30	Depth	Laingsburg	33.256	20.851	776	1.6	0.99	0.73
SA-LB_DP85	Depth	Laingsburg	33.256	20.851	776	1.6	0.99	0.41
SA-LB_DP150	Depth	Laingsburg	33.256	20.851	776	1.6	0.99	0.21
SA-LB_DP255	Depth	Laingsburg	33.256	20.851	776	1.6	0.99	0.07

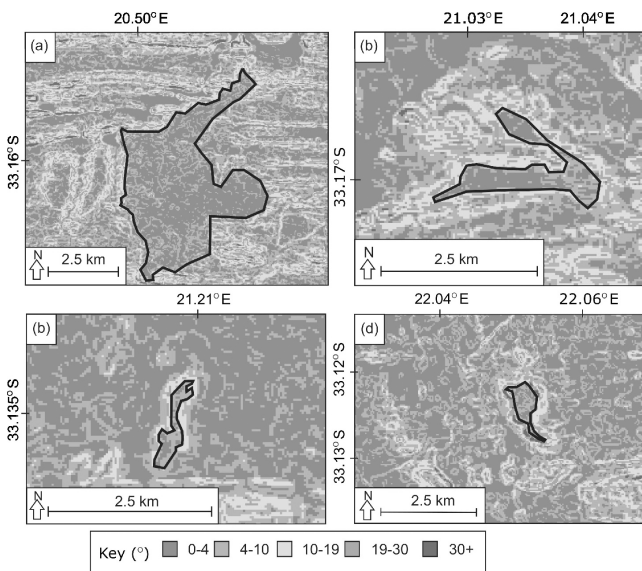


Figure 5. Pediment slope data (with slope given in °): (a) Laingsburg, (b) Floriskraal, (c) Leeuwgat and (d) Prince Albert. For pediment locations please see Fig. 4.

nominal ratio of 28.1×10^{-12} (Kubik and Christl, 2010), which is in agreement with a ¹⁰Be half-life of 1.387 Myr (Chmeleff et al., 2010). Sample ratios were blank corrected $(7.54 \pm 9.67) \times 10^{-15}$, and the analytical uncertainties on the ¹⁰Be/⁹Be ratios of blanks and samples were then propagated into the 1σ analytical uncertainty for the ¹⁰Be concentrations (Tables 2 and 3). Production rates were scaled following Dunai (2000) with a sea level high-latitude production rate of 4.28 atoms g⁻¹qtz yr⁻¹. The bulk density was set to 2.7 g cm⁻³ for samples from quartzite boulders following Scharf et al. (2013) and to 1.6 g cm⁻³ for the overburden of the depth samples following earlier work on depth profiles

Table 2. Cosmogenic nuclide data for a depth profile in Laingsburg. The reported ¹⁰Be concentrations are corrected for procedural blanks using a value of $(7.54 \pm 9.67) \times 10^{-15}$, and the 1σ uncertainty estimates contain analytical errors from accelerator mass spectrometer (AMS) measurement and blank error propagation.

Sample ID	Depth (cm)	¹⁰ Be concentration (±1σ) (atoms g ⁻¹ qtz)
SA-LB_DP0	0	$(5.46 \pm 0.11) \times 10^6$
SA-LB_DP30	30	$(1.20 \pm 0.11) \times 10^6$
SA-LB_DP85	85	$(8.93 \pm 0.36) \times 10^5$
SA-LB_DP150	150	$(3.76 \pm 0.16) \times 10^5$
SA-LB_DP255	255	$(1.33 \pm 0.15) \times 10^5$

in the Western Cape by Kounov et al. (2015). The concentrations were corrected for topographic shielding using the procedure described in Norton and Vanacker (2009).

For the derivation of the minimum durations of exposure (Table 3), we used two different scenarios: a hypothetical case assuming no erosion or burial since exposure and a second case assuming steady erosion of the pediment surface of 0.3 m Myr⁻¹ following Bierman et al. (2014). The CosmoCalc method version 3.0 (Vermeesch, 2007) was employed to calculate maximum denudation rates and minimum surface exposure ages from the ¹⁰Be concentrations of the surface samples (Table 3). The surface exposure ages are *minimum estimates* as isotopic steady state can be reached for old material.

In addition, we use a concentration depth profiling approach to better constrain the exposure and denudation of the Laingsburg area pediment. The accumulation of ¹⁰Be, $N_{total}(z, t)$, in the eroding surface of the pediments can be



Figure 6. (a) Sedimentary log of the Laingsburg pediment showing the unsorted boulder- (dominantly quartzite) to gravel-sized material; (b) photograph of the pediment and where the depth profile clasts were taken; (c) iron-rich palaeosol layer.

Table 3. Cosmogenic nuclide data for surface samples from pediments. The reported ^{10}Be concentrations are corrected for procedural blanks, using a value of $(7.54 \pm 9.67) \times 10^{-15}$, and the 1σ uncertainty estimates contain analytical errors from AMS measurement and blank error propagation. Maximum denudation rates and minimum durations of surface exposure were calculated using the CosmoCalc add-in for Excel (Vermeesch, 2007). For the surface exposure ages (T_{exp}), we assumed (1) no erosion or burial since exposure and (2) a maximum steady erosion rate of 0.3 m Myr^{-1} .

Sample ID	Location	^{10}Be concentration (atoms $\text{g}_{\text{qtz}}^{-1}$) ($\pm 1\sigma$)	^{10}Be denudation rate (m Myr^{-1}) ($\pm 1\sigma$)	Minimum exposure age (yr) ($\pm 1\sigma$)	
				No erosion or deposition	Erosion rate of 0.30 m Myr^{-1}
SA-PA_ped	Prince Albert	$(2.83 \pm 0.06) \times 10^6$	0.954 ± 0.025	$(5.69 \pm 0.10) \times 10^5$	$(6.78 \pm 0.10) \times 10^5$
SA-LB_ped1	Laingsburg	$(5.20 \pm 0.10) \times 10^6$	0.408 ± 0.013	$(1.13 \pm 0.02) \times 10^6$	$(1.96 \pm 0.02) \times 10^6$
SA-LB_ped2	Floriskraal	$(5.15 \pm 0.10) \times 10^6$	0.383 ± 0.013	$(1.19 \pm 0.02) \times 10^6$	$(2.22 \pm 0.02) \times 10^6$
SA-LB_ped3	Leeuwgat	$(5.64 \pm 0.10) \times 10^6$	0.315 ± 0.011	$(1.38 \pm 0.02) \times 10^6$	$(4.46 \pm 0.02) \times 10^6$
SA-LB_ped4	Laingsburg	$(4.25 \pm 0.07) \times 10^6$	0.587 ± 0.014	$(8.48 \pm 0.11) \times 10^5$	$(1.16 \pm 0.01) \times 10^6$
SA-LB_DP0	Laingsburg	$(5.46 \pm 0.11) \times 10^6$	0.373 ± 0.013	$(1.21 \pm 0.02) \times 10^6$	$(2.33 \pm 0.02) \times 10^6$

described as

$$N(z, t) = N_{\text{inh}} e^{-\lambda t} + \sum_i \frac{P_i(z)}{\lambda + \frac{\rho E}{\Lambda_i}} e^{-\rho(z_0 - Et)/\Lambda_i} \left(1 - e^{-\left(\lambda + \frac{\rho E}{\Lambda_i}\right)t} \right), \quad (1)$$

where E is expressed in centimetres per year (cm yr^{-1}) ($\text{m Myr}^{-1} \times 10^4$) and t (yr) is the exposure age, λ (yr^{-1}) the nuclide decay constant ($\lambda = \ln 2/t_{1/2}$), z_0 (cm) the initial shielding depth ($z_0 = E \times t$), ρ (g cm^{-3}) the density of the overlying material and Λ_i (g cm^{-2}) the attenuation length. The production rate, $P_i(z)$ (atoms $\text{g}_{\text{qtz}}^{-1} \text{ yr}^{-1}$), is a function of the depth, z (cm), below the surface. The subscript “ i ” indicates the different production pathways of

^{10}Be via spallation, muon capture and fast muons following Dunai (2010). In this study, the relative spallogenic and muogenic production rates are based on the empirical muogenic-to-spallogenic production ratios established by Braucher et al. (2011) using a fast muon relative production rate at sea level and high latitude (SLHL) of 0.87 % and slow muon relative production rate at SLHL of 0.27 %. The attenuation length was set to 152, 1500 and 4320 g cm^{-2} for the production by, respectively, neutrons, negative muons and fast muons (Braucher et al., 2011). The depth profile is then solved numerically, based on model fitting between the observed (Table 2) and simulated ^{10}Be concentrations at different depths for a wide range of exposure age (T_{exp} , 0.4

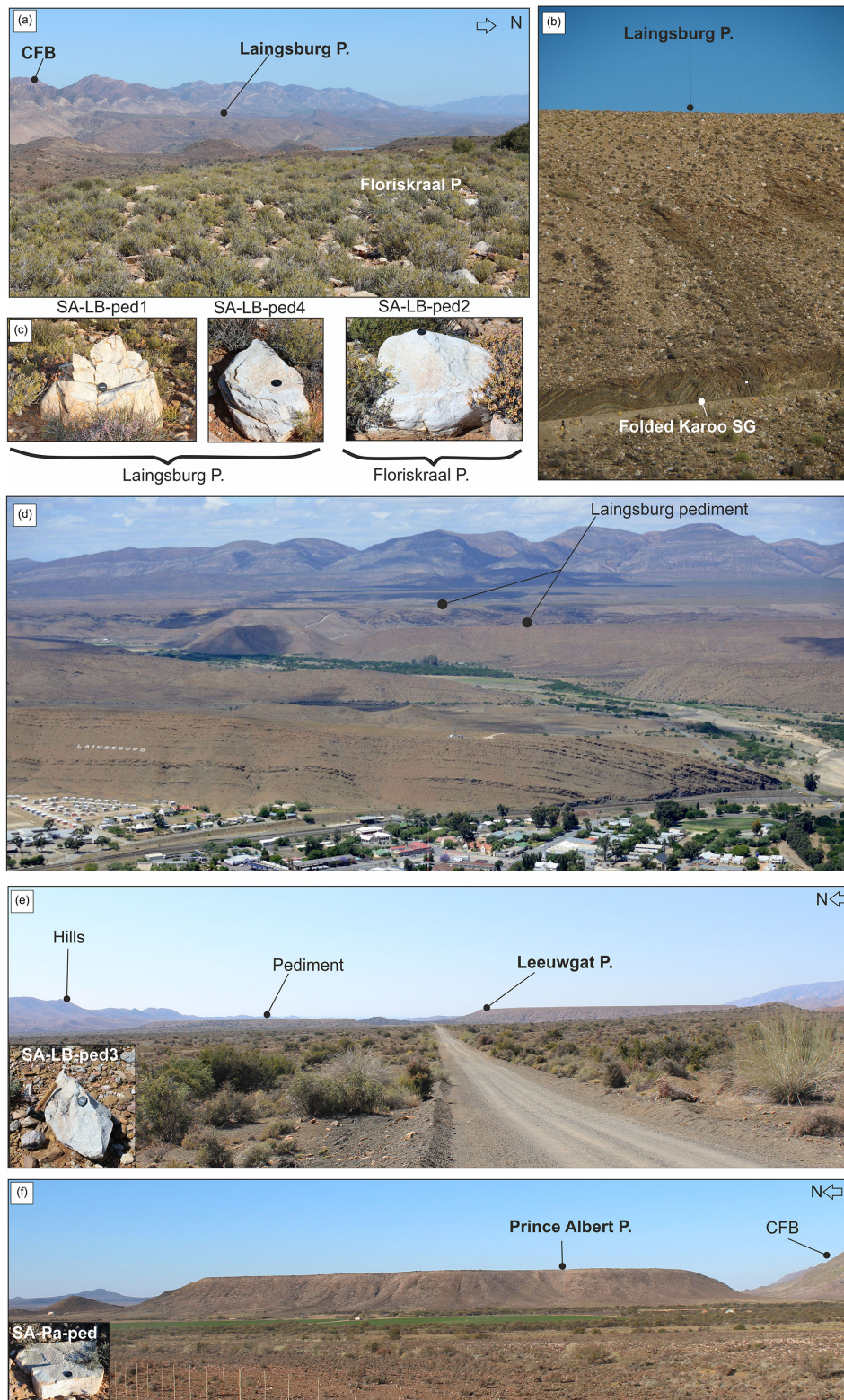


Figure 7. Sample sites. (a) Laingsburg pediment from the Floriskraal pediment; (b) Laingsburg pediment and contact with underlying folded Karoo Supergroup (SG) strata; (c) boulder samples from Laingsburg and Floriskraal pediments; (d) large-scale picture of the Laingsburg pediment; (e) Leeuwgat pediment and boulder sample (inset); (f) Prince Albert and boulder sample (inset). The figure also shows the dissection of the pediments by small river catchments and how decoupled the Floriskraal and Prince Albert pediments are from the Cape Fold Belt.

to 20 Ma), denudation rate (0 to 1.5 m Myr⁻¹), inheritance ($N_{\text{inh}}e^{-\lambda t} = N_{255\text{cm}}$ vs. no inheritance) and deflation scenarios. The Nash–Sutcliffe efficiency and the χ^2 were used to assess the predictive power of the numerical models following Vandermaelen et al. (2022).

3.2 Morphometric analysis

Aster 30 m data were used to build a DEM of the study area in ArcGIS 10.1. The DEM was re-projected into WGS 1984 world Mercator coordinates, and gaps were filled using the hydrology toolbox. The drainage was extracted using an upstream contributing area of 3.35 km², and both ephemeral and perennial streams were delineated (e.g. Abadelkaarem et al., 2012; Ghosh et al., 2014). Dissected pediments were derived using a method adapted from Bellin et al. (2014). The previous grading from the mountain front was reconstructed for each pediment in ArcGIS (Fig. 8). This surface was then placed into ArcScene 10.1, with the difference between the reconstructed surface and the current topography (using the DEM) providing a minimum volume of material removed after pediment formation. A similar approach was applied to derive bulk erosion volumes for the small sub-catchments that back the pediment surfaces in the CFB. The bulk erosion is likely to be a minimum estimate of the total rock volume removed by erosion, as interfluvial erosion might have occurred (Bellin et al., 2014; Brocklehurst and Whipple, 2002). Eroded volumes were then converted to lithological thickness using the method of Aguilar et al. (2011).

4 Results

4.1 Alluviated pediment composition

The contact with the underlying bedrock (e.g. Dwyka Group) is erosional and undulating; it is not a smooth planation contact. The alluviated pediments are composed of poorly sorted boulders to pebbles, with a matrix of sandy gravel. The clasts are predominantly quartzites (Table Mountain Group); however smaller clasts of Dwyka Group lithologies are present. Towards the top of the profile there is a small transition zone of gravel, which is capped by an iron crust (Fig. 6). There is no indication of fluvial activity (i.e. imbrication). There is no grading or sediment clast size variation throughout the profile, and the clasts range from sub-rounded to sub-angular.

4.2 Cosmogenic nuclides

The concentrations of ¹⁰Be produced in situ in boulders sampled on the pediment surface range between $(2.83 \pm 0.06) \times 10^6$ and $(5.64 \pm 0.10) \times 10^6$ atoms g_{qtz}⁻¹. The CRN concentrations are indicative of old surfaces with very low denudation, and we obtained long-term denudation rates of 0.315 to 0.954 m Myr⁻¹ for the pediments. The alluviated pediment in the Prince Albert area has the highest rate of

maximum surface lowering (0.954 m Myr⁻¹), which is an order of magnitude higher than the average surface lowering rate of the pediments in the Laingsburg area. In the latter area, the surface denudation rates decrease from the CFB towards the proximal part of the pediment (Table 3).

The alluviated pediments are long-lived and have been exposed for at least 0.678 to 4.46 Myr (when we assume that the surface was lowered by ~ 0.3 m Myr⁻¹). The CRN depth profile in the Laingsburg pediment demonstrates the existence of a deflation surface as result of differential erosion. The profile consists of five samples, taken at the surface and 30, 80, 150 and 255 cm depths. The ¹⁰Be concentrations steadily decrease with depth (Fig. 9a), whereby the ¹⁰Be concentration of four lower samples decreases exponentially with depth, as theoretically expected for cosmogenic radionuclide production by neutrons with a fitted exponent of -0.01 ($N_{10\text{Be}} \approx e^{-0.01 \times \text{depth}}$, RMSE = 1.49×10^5 atoms g_{qtz}⁻¹) corresponding well to an attenuation length of 160 g cm⁻² for a matrix density of 1.6 g cm⁻³. In contrast, the top sample (SA-LB-DP0) has a concentration that is more than double the theoretically expected ¹⁰Be concentration (Table 3). We attribute this phenomenon to surface deflation: boulders covering the ground surface are part of a deflation armour and are exposed longer to cosmic rays than the matrix of sandy gravel in which they are now embedded. Based on the exponential fit through the four lowermost data points, we estimate that ~ 110 cm of fine-grained matrix was removed from the top of the pediment by deflation (Fig. 9b) resulting in a pavement of old boulders at the top of a slowly eroding surface (Fig. 10).

Based on Eq. (1), we modelled the ¹⁰Be concentration depth profile of the Laingsburg pediment for a wide spectrum of possible erosion–exposure age scenarios. We evaluated the goodness of fit of the predicted models based on the Nash–Sutcliffe efficiency (NSE) and χ^2 (Fig. 11). Our results show no significant improvement in model performance when accounting for inheritance, indicating that inheritance can be neglected in the analyses of the ¹⁰Be depth profiles in the Laingsburg pediment. Otherwise, deflation of the surface is confirmed by the simulation outcomes because (i) model predictions using erosion–exposure age scenarios that disregard deflation all have an NSE below 0.60, while their corresponding scenarios accounting for deflation armouring have an NSE up to 1.00, and (ii) a two-sample comparison *t* test confirms significantly lower fit for model predictions that disregard deflation.

Optimal model fits, defined as model predictions with an NSE approaching 1 and minimal χ^2 value, are obtained for the scenarios with long-term erosion between ~ 0.3 and 0.6 m Myr⁻¹ and exposure exceeding ~ 2 Myr. Not only is this result congruent with the outcomes of the CosmoCalc method (Table 3), it also provides more details on the erosion–exposure scenarios that are most likely to explain the long-term evolution of the pediment.

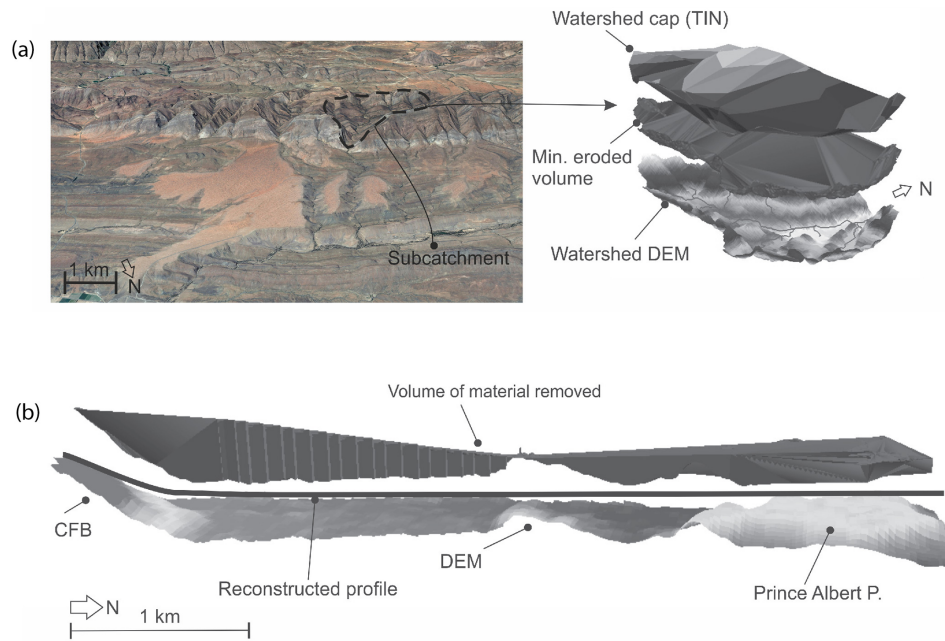


Figure 8. Examples of (a) bulk eroded volumes from sub-catchments and (b) cross section of the Prince Albert pediment showing the method used in ArcGIS for the volume of material removed around the pediment surface. Imagery for (a) from © Google Earth 2015.

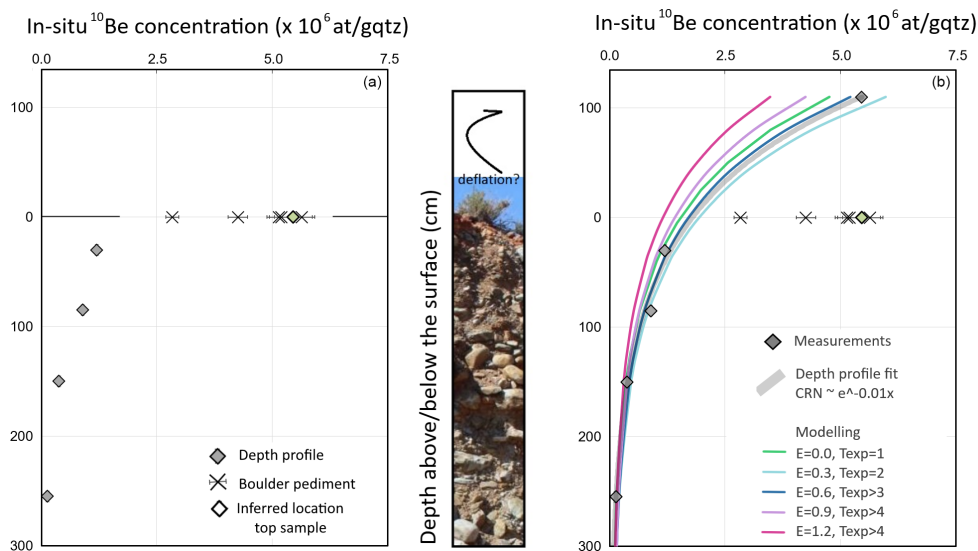


Figure 9. Depth profile in the Laingsburg pediment. Panel (a) shows in situ ^{10}Be concentrations (expressed in atoms of ^{10}Be per gram of quartz) as measured in depth profile and boulders from other pediments listed in Table 3. (b) Modelled in situ ^{10}Be concentration from a data-fitted exponential model ($N_{^{10}\text{Be}} \approx e^{-0.01 \times \text{depth}}$) and from numerical simulations using forward modelling for given erosion rates (E expressed in m Myr^{-1}) and exposure ages (T_{exp} expressed in Ma). For erosion rates exceeding 0.6 m Myr^{-1} , the in situ ^{10}Be concentrations are in secular equilibrium for exposure ages exceeding the T_{exp} indicated in the graph, and the concentration depth profiles become time-invariant.

4.3 Elevations and grading of pediment

Figure 4c shows the pediment heights as classified by the Jenks natural break scheme (De Smith et al., 2007). The alluviated pediments at Laingsburg and Floriskraal have elevations within the same class (714–870 m), and the Leeuw-

gat and Prince Albert area alluviated pediments share the same elevation class (617–713 m). The Laingsburg area alluviated pediment appears to have an aspect of slope that grades not only away from the CFB but towards the modern Buffels River location, which abuts the northern limit of the

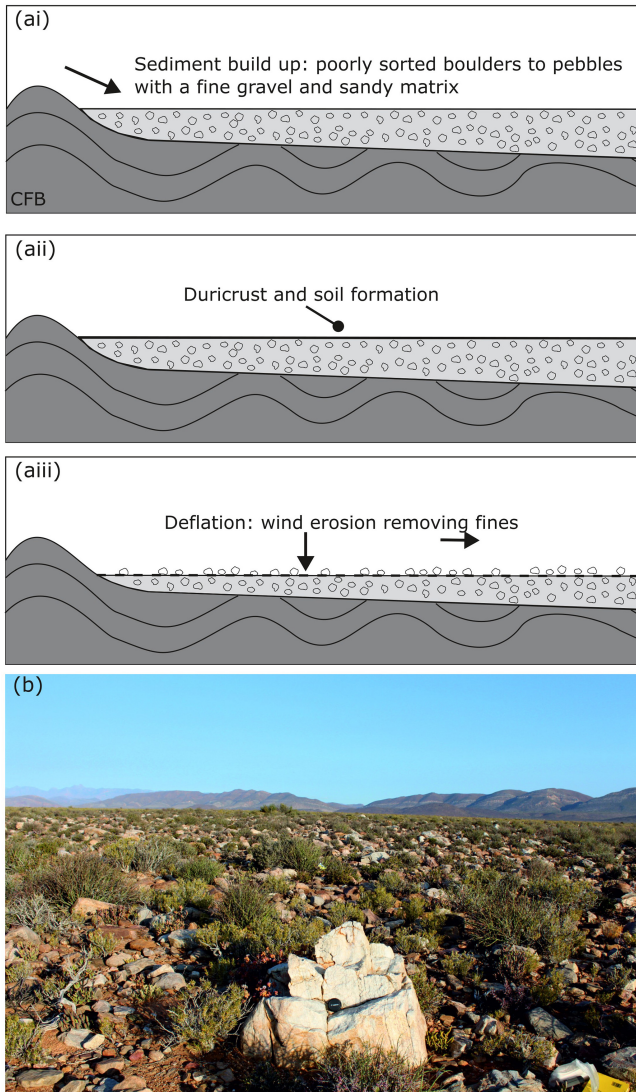


Figure 10. (a) Process of deflation and (b) evidence of deflation: concentrations of boulders and pebbles on top of the Laingsburg Pediment.

alluviated pediment (Fig. 12). This relationship is less clear on the Floriskraal alluviated pediment, which is to the east of the Buffels River. The alluviated pediment at Leeuwgat, which sits between two folds of the CFB, has no large trunk river nearby (~ 30 km from Dwyka River) and simply grades away from the CFB (Fig. 13a). The Prince Albert area pediment grades towards the Gamka River, although it is currently ~ 16 km from the Gamka River (Fig. 13b). The fact that the alluviated pediments grade towards the present-day trunk rivers but above their present-day elevation indicates that these rivers were active during the formation of the pediments and is discussed later.

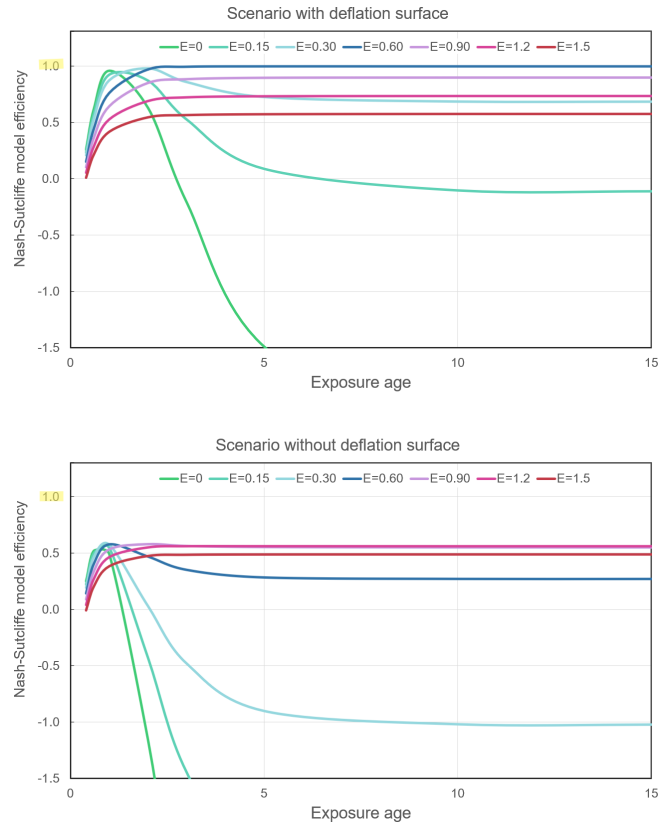


Figure 11. Goodness of fit of the model predictions for the ^{10}Be depth concentration profile in the Laingsburg pediment, as evaluated by the Nash–Sutcliffe efficiency (NSE). The NSE ranges between $-\infty$ and 1, whereby 1 corresponds to a perfect model fit. Model simulations were realised for a wide range of exposure ages (0 to 20 Ma) and denudation rates ($E = 0$ to 1.5 m Myr^{-1}) and for conditions with and without inheritance ($N_{\text{inh}}e^{-\lambda t} = N_{255 \text{ cm}}$) and deflation armouring. For simulations with the development of armouring, optimal solutions ($\text{NSE} \rightarrow 1$) are found for denudation between 0.3 and 0.6 m Myr^{-1} and exposure ages exceeding 2 Ma . Model performances for simulations neglecting surface deflation are significantly lower ($\text{NSE} \rightarrow 0.6$), illustrating the necessity to account for deflation armouring.

4.4 Dissecting river planform

The dissecting river planforms are shown in Fig. 14. Critical points are highlighted that relate to sections where the rivers (i) have been deflected by the pediment surface or (ii) have anomalous changes in orientation. Overall, the low-order rivers (< 4) that have dissected the pediments are strongly influenced by the folding within the CFB (Richardson et al., 2016). This is especially seen within the rivers that have dissected the Laingsburg pediment (Fig. 14a), where the linear river planform aligns with the axis of a syncline. Where the rivers breach a fold, it appears that the presence of alluviated pediments deflected the river planforms; this relationship can also be seen in the alluviated pediments in the Floriskraal and Prince Albert areas (Fig. 14).

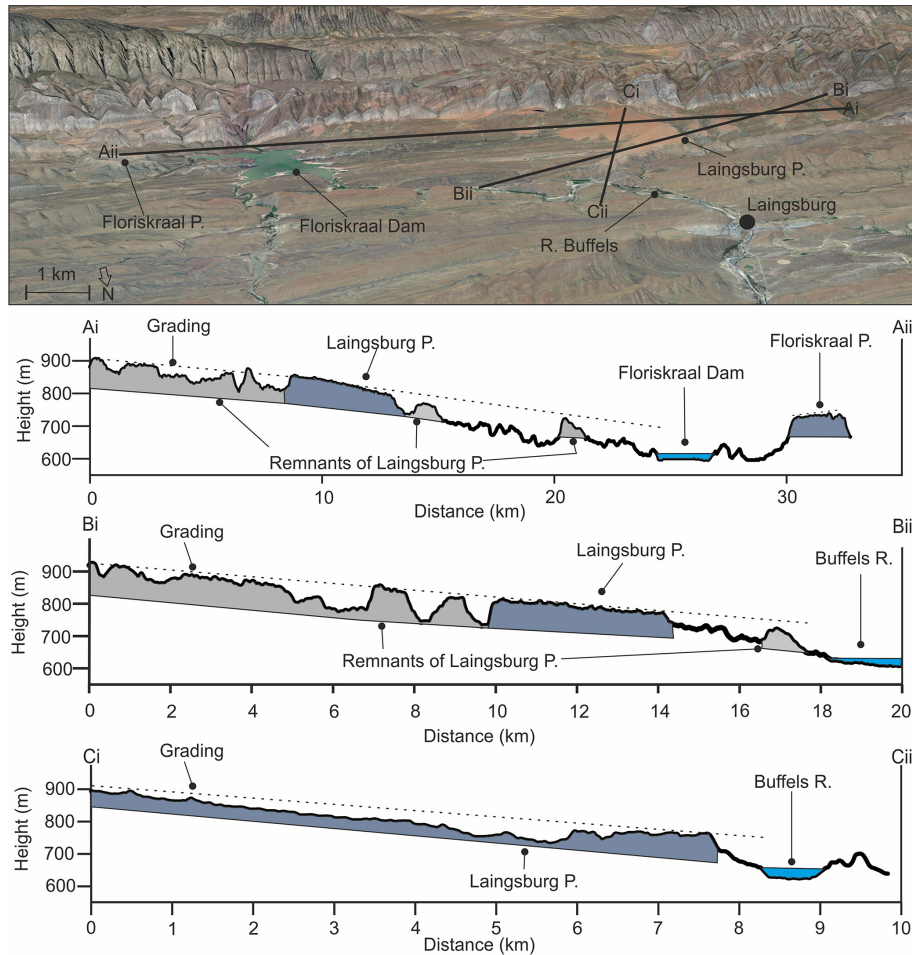


Figure 12. Grading of the Laingsburg pediment and related cross sections, which grade not only away from the Cape Fold Belt but towards the Buffels River. Imagery from © Google Earth 2015.

4.5 Volume of material removed

Table 4 shows the bulk erosion rates related to the dissection of the alluviated pediments post-formation. Converting this to an equivalent lithological thickness (dividing the volume of material removed over the area; Aguilar et al., 2011), an average of 141 m has been eroded around the large Laingsburg area pediment (Fig. 12). The Prince Albert area pediment has an average lithological thickness of 42.3 m removed. Leeuwgat has had the least amount of dissection, with 17.3 m eroded.

Table 5 shows the volume of material eroded by rivers draining the sub-catchments in the CFB, which have dissected the alluviated pediments. The sub-catchments range in size from < 5 to 310 km², and the volume of material removed ranges from < 0.1 to 89 km³, which is the equivalent of ~ 20 to 286 m of lithological thickness. The alluviated pediments that are located further away from the CFB range have larger dissecting catchments associated with them. For example, the Laingsburg area alluviated pediment, which is

Table 4. Minimum volume of material eroded by rivers incising the pediment surface, the equivalent rock thickness and the time taken for incision using the average maximum denudation rate of 10.2 m Myr⁻¹ from Scharf et al. (2013) and Kounov et al. (2015).

Location	Volume of material removed (km ³)	Equivalent average rock thickness (m)	Time for incision (yr)
Laingsburg	3.24	1.41 × 10 ²	1.39 × 10 ⁷
Floriskraal	1.54 × 10 ⁻¹	4.23 × 10 ¹	4.17 × 10 ⁶
Leeuwgat	1.69 × 10 ⁻¹	4.43 × 10 ¹	4.36 × 10 ⁶
Prince Albert	1.20 × 10 ⁻²	1.73 × 10 ¹	1.70 × 10 ⁶

backed by the CFB, has an average sub-catchment area of ~ 14 km², whereas the Prince Albert area alluviated pediment is located ~ 2 km from the CFB and has an average sub-catchment area of ~ 162 km². These sub-catchment areas are contributing to the incision of the pediments.

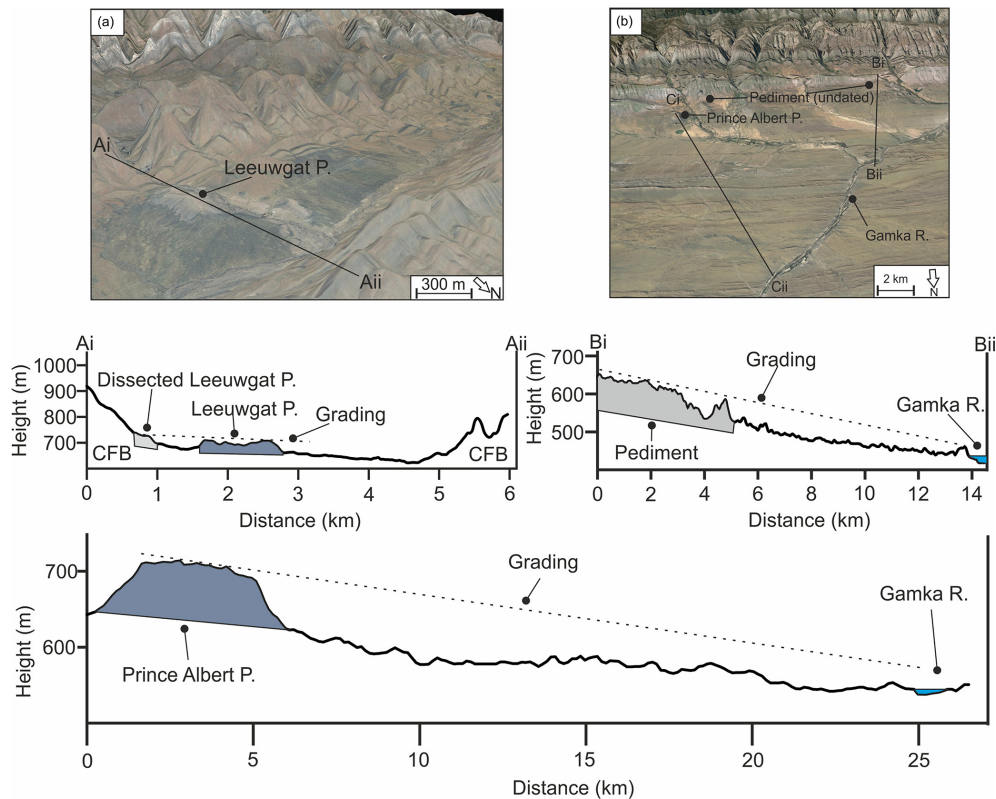


Figure 13. Grading of the (a) Leeuwgat, which grades away from the Cape Fold Belt, and (b) Prince Albert pediment, which grades towards the Gamka River. Imagery in (a) and (b) from © Google Earth 2015.

Table 5. Minimum volume of material eroded by rivers draining the Cape Fold Belt sub-catchments, the equivalent rock thickness and the average time taken for incision using the average of the maximum denudation rate recorded from Scharf et al. (2013) and Kounov et al. (2015) of 10.2 m Myr^{-1} .

Location	Catchment	Area (km^2)	Volume of material removed (km^3)	Equivalent average rock thickness (m)	Time for incision (yr)
Laingsburg	CFB 1	1.98×10^1	2.86	1.44×10^2	1.42×10^7
	CFB 2	8.96	8.47×10^{-1}	9.56×10^1	9.40×10^6
Floriskraal	CFB 3	6.21	2.82×10^{-1}	4.53×10^1	4.46×10^6
	CFB 4	6.02	2.02×10^{-1}	3.36×10^1	3.31×10^6
Leeuwgat	CFB 5	7.38×10^1	7.55	1.02×10^2	1.01×10^7
	CFB 6	4.91	1.06×10^{-1}	2.16×10^1	2.13×10^6
Prince Albert	CFB 7	3.11×10^2	8.90×10	2.86×10^2	2.82×10^7
	CFB 8	1.29×10^1	2.30×10^{-1}	1.78×10^1	1.75×10^6

5 Discussion

5.1 Pediment formation and characteristics

The pediments are underlain by folded strata of the Karoo and Cape supergroups (sandstone, siltstone and mudstone) and backed by the resistant CFB quartzites (Fig. 4b). It has been argued that pediments form on all lithology types; how-

ever the more extensive pediments can be found on less resistant material (Dohrenward and Parsons, 2009). There is no systematic variation in pediment characteristics that can be related to the underlying geology (Fig. 4b).

The pediments have formed by diffusive processes, dominated by slope processes in the first stages of development, causing the gradual retreat of the Cape Fold Belt and coeval formation of colluvial material and weathering mantle, in-

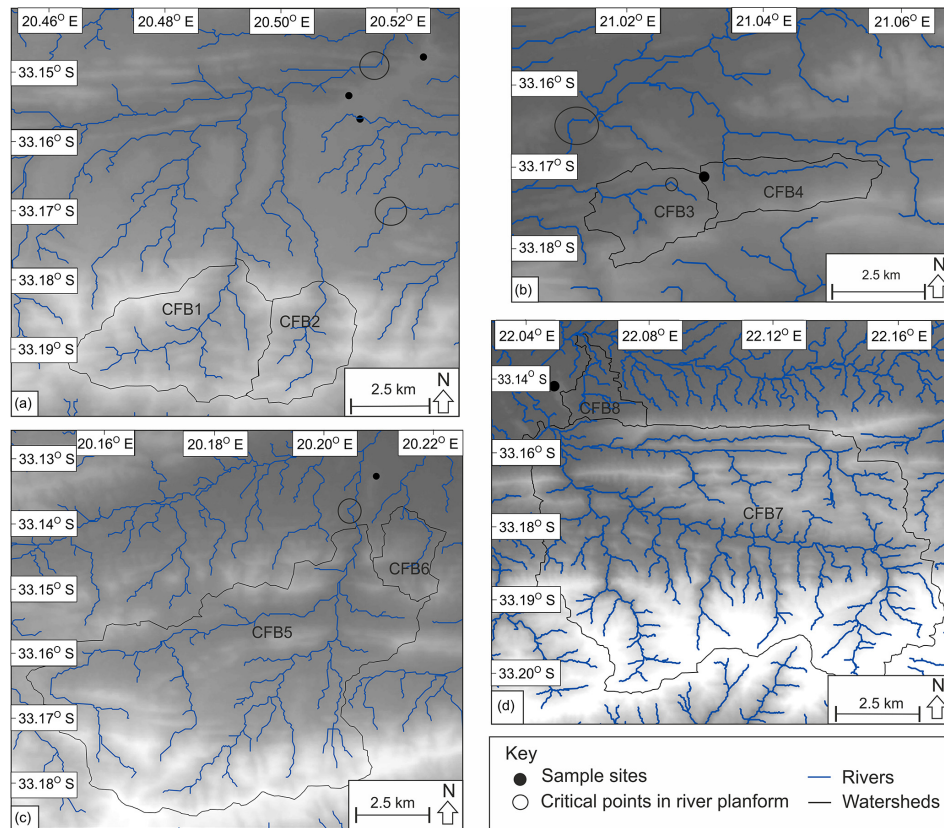


Figure 14. Planforms of the dissecting rivers and Cape Fold Belt sub-catchments: (a) Laingsburg, (b) Floriskraal, (c) Leeuwgat and (d) Prince Albert. The circles highlight critical points related to the deflection of the river planforms by the Cape Fold Belt or the pediment.

cluding an iron pan (Fig. 15). There is no evidence of fluvial activity, such as clast imbrication, depositional or erosional bedforms, or channel forms (Fig. 6; cf. e.g. Gilbert, 1877; Sharp, 1940; Lustig, 1969). The iron pan layer is now at the surface of the pediment due to the removal of overlying material as a result of surface deflation by wind erosion, as shown by the cosmogenic data from the ^{10}Be concentration depth profile (Figs. 9, 15). The pediments grade towards, but above, large trunk rivers of the Gouritz catchment (Figs. 12, 13), indicating that large transverse systems were active before pediment planation and colluvial build-up. The trunk rivers were also active during pediment formation; however they were probably less so, as shown by the build-up and preservation of material forming the pediments. This suggests that at the time of pediment formation there was deposition of colluvial material adjacent to large-scale sediment bypass via rivers and the formation of the pediment surfaces because of erosion processes. The trunk rivers, active during the formation of the pediments, represent an upper limit to the extent of the pediments, and the pediments should be regarded as individual landforms and not as an extensive regional “surface” within the study area (cf. King, 1948, 1953, 1955; Partridge and Maud, 1987).

The distribution of the dissected pediments suggests that these are remnants of much more continuous local features (Fig. 13). There has been a shift in the dominant process regime, from slope processes to fluvial processes, during the evolution of the pediments as evidenced by the dissection of pediments by smaller rivers and the decoupling of the pediments from the CFB sediment source area. The river planform has been primarily controlled by the orientation of tectonic folds. However, the pediments could have also controlled the landscape evolution by deflecting the rivers, allowing the surfaces to be preserved. It appears that the structural integrity of the pediment is not continuous across the entire pediment. Areas underlain by cohesive material caused deflection of the dissecting rivers due to a higher resistance to erosion (Fig. 14). This could be a function of the sedimentology (Fig. 6) of the pediment: the calibre of material, the extent of packing, or the presence and thicknesses of the duricrust layer. Deflection of rivers has been shown to cause the formation of epigenetic gorges (Ouimet et al., 2008). Furthermore, the pediments could have been preserved in these locations as rivers did not migrate laterally, which could be due to variations in channel gradient. The pediments sit above the valley floor (current level of erosion) and are fossilised landforms that represent a store of sediment that is mostly subject

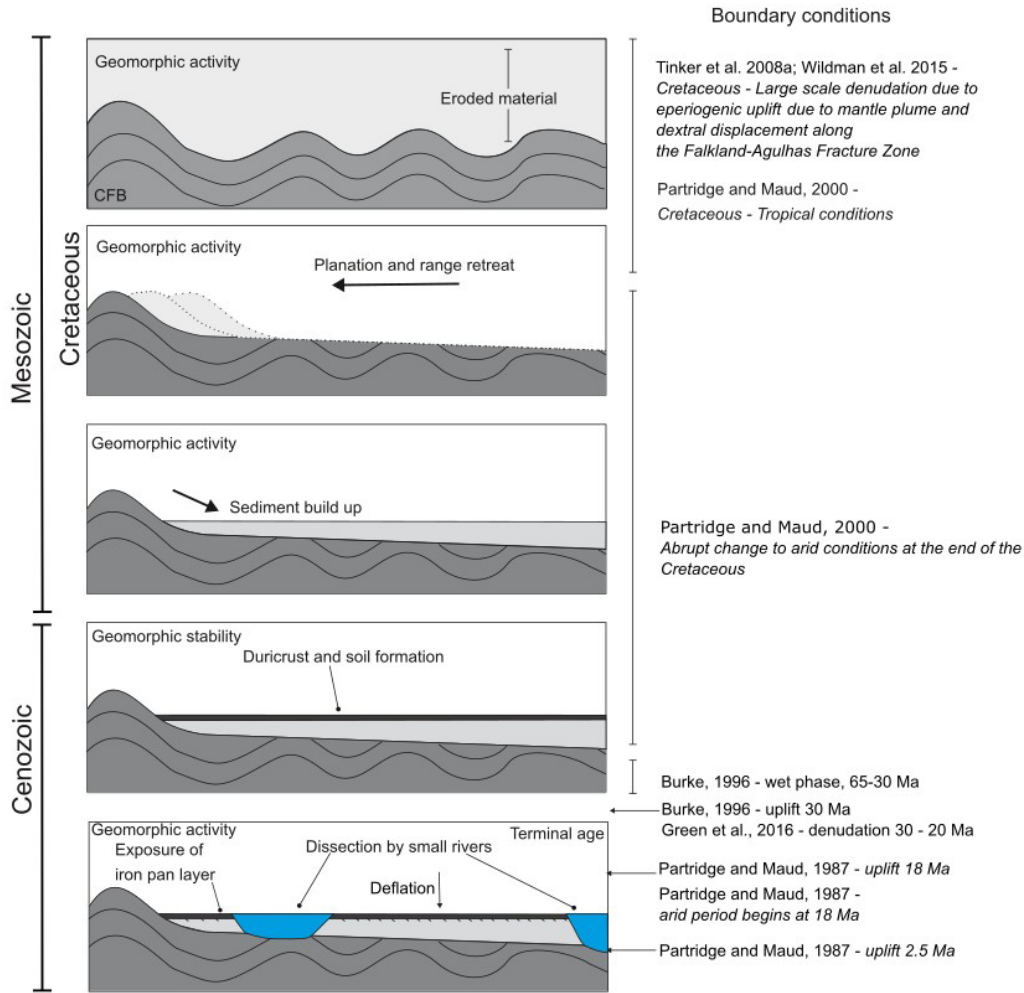


Figure 15. Sequence of events forming the pediments and boundary conditions, in which the folded Karoo Supergroup strata were planed and hillslope processes caused the build-up of sediment, soil formation and duricrust formation. The pediments were then dissected, and fluvial processes dominate. In recent time, deflation processes have dominated (Fig. 10).

to slow denudation and weathering, followed by deflation under current climatic conditions (Fig. 10). Hillslope processes have slowly supplied sediment to the nearby fluvial channels; however due to slow runoff rates related to the arid climate, the transport is no longer effective.

5.2 Implications of depth profile

The ¹⁰Be concentration depth profile (Fig. 9a) in the Laingsburg pediment deviates from a simple exponential concentration depth profile. The stronger than theoretically expected decrease in ¹⁰Be concentrations in the upper 30 cm points to a complex post-depositional history of the alluviated pediment. The deviation can be explained by a long phase of low denudation rate (0.3 to 0.6 m Myr⁻¹) followed by aeolian deflation whereby finer material is preferentially removed. Deflation has been reported for (semi-)arid environments during the Cenozoic (Binnie et al., 2020). The impact of defla-

tion on ¹⁰Be concentrations has been described for glacial outwash terraces (Hein et al., 2009; Darvill et al., 2015) where aeolian deflation and bio- or cryoturbation caused previously buried cobbles to become exposed. It has also been recorded for periglacial areas of central Europe where depth profiles revealed denudation rates of 40 to 80 m Myr⁻¹ during the Quaternary (Ruszkiczay-Rüdiger et al., 2011). Binnie et al. (2020) showed that deflation on marine terraces in northern Chile is the primary cause for multimodal distributions of ¹⁰Be concentration depth profiles. Although the climate in southern South Africa has become more arid since the Cenozoic, the impact of aeolian deflation on ¹⁰Be concentrations of pediment surfaces has not yet been addressed in previous work. Further work is needed to understand if this behaviour is apparent across other pediment surfaces in the area and how common this feature is across other pediment surfaces.

Our results also warrant caution for potential bias that can arise when collecting only surface samples from alluvial pediments. Boulders armouring the surface of alluvial pediments can be enriched in ^{10}Be concentrations compared to the sandy matrix, as they are residual features. Their concentrations of ^{10}Be produced in situ are pertinent to reconstructing exposure ages but underestimate surface process rates. In contrast, sampling sand-sized material from the surface would have yield erroneous inferred ages that are too young (Fig. 9b). There is an added value in sampling pediments at a minimum of three depths covering a full path attenuation length, as additional information on erosion–exposure age scenarios can be provided.

5.3 Geomorphic, tectonic, climatic and stratigraphic considerations

The cosmogenic data presented in Table 3 and Fig. 9 are within the range of data presented in Fig. 3 (van der Wateren and Dunai, 2001; Bierman et al., 2014; Kounov et al., 2015). There is no systematic spatial variation in surface lowering rates of the pediments that can be correlated to pediment size or geology. The Prince Albert area alluviated pediment is the most isolated from the CFB, with no duricrust present (Fig. 4a), which can explain why the surface lowering rates are the highest in this location (0.954 m Myr^{-1} compared to a maximum of 0.587 m Myr^{-1} for the other pediments). Further, the pediment surfaces only remain fossilised as long as the duricrust remains. When the duricrust is removed, denudation rates likely increase slightly as shown by the Prince Albert area alluviated pediment but will still remain low compared to other landforms (Fig. 3, Table 3). Therefore, the duricrusts represent an intrinsic geomorphic threshold. Using forward modelling on the depth profile in the Laingsburg pediment, we demonstrated that the ^{10}Be concentrations are at secular equilibrium and that the pediment has been exposed for more than 2 Myr (Fig. 11).

The volume of material removed by river incision into the pediment surfaces equates to a lithological thickness of ~ 42 to 141 m (Table 4). Assuming an average maximum denudation rate of the surrounding CFB area (10.2 m Myr^{-1} from Scharf et al., 2013, and Kounov et al., 2015), we can estimate that the dissection started as early as ~ 2 to 14 Myr ago. Cosmogenic and thermochronological (apatite fission track and (U–Th) / He) studies have reported low denudation rates across the Cenozoic, and Scharf et al. (2013) stated that the close agreement between the CRN-based denudation and apatite fission track analysis (AFTA) / (U–Th) / He exhumation rates is indicative of relative tectonic stability over the last 10^6 to 10^8 years.

As the dissection would have occurred after the formation of the alluviated pediments, they need to be older than the start of the incision phase (2–14 Myr). Based on the observed denudation of the sub-catchments within the CFB that back the pediments and the mean maximum denudation rates from

Scharf et al. (2013) and Kounov et al. (2015) (Figs. 3 and 8, Table 5), we obtain indicative minimum ages of 9–14 Ma for the Laingsburg area pediment, 3–4 Ma for Floriskraal, 2–10 Ma for Leeuwgat and 2–28 Ma for Prince Albert. The CFB sub-catchment denudation ages represent the ages of the dissecting rivers reaching the CFB after dissecting the pediment surfaces. These indicative ages must be taken with caution as maximum published rates have been used, and denudation rates vary over time, with a phase of increased erosion likely forming the incised channels. Furthermore, as shown by the pediments causing the deflection of surrounding rivers (Fig. 14), denudation of the pediment is slow (estimated between 0.3 and 0.6 m Myr^{-1}) as the resistance of the pediment is higher than the surrounding bedrock in some locations.

Using a combination of the data above, including data on the dissection of the pediment and backing sub-catchments eroded into the resistant Cape Fold Belt catchments, the Laingsburg area pediment could have an age of 23 Ma, Floriskraal 8 Ma, Leeuwgat 10 Ma and Prince Albert 17 Ma. These age estimates correspond to the start of dissection and are based on the assumption that geomorphic process rates were steady over long timescales. The geomorphic evidence corroborates the outcomes of the numerical simulations of possible erosion–exposure age scenarios for the Laingsburg pediment, uncovering the possibility of having very old (3 to > 15 Myr) exposed surfaces. If the cosmogenic *minimum* exposure ages are used, with the volume eroded recorded using the DEM, erosion rates range from 28 to 503 m Myr^{-1} , which further indicates the minimum exposure ages should be taken with caution as these extremely high erosion rates have not been recorded using published studies (Fig. 3). Previous works have classified pediment surfaces within height brackets (e.g. King, 1953). However, in this study there is no correlation between pediment elevation and their geomorphic ages.

Duricrusts are found in many of the studied alluviated pediments (Summerfield, 1983; Marker et al., 2002), and this is well-developed in the Laingsburg area pediment (Fig. 5). The alluviated pediments no longer have the overlying weathering material preserved and have been lowered to the iron pan layer. The depth profile suggests that erosion has occurred after the development of the weathering mantle (Fig. 9), which has exposed the iron pan (laterites). The iron pan could have formed by leaching from surrounding lithologies and clasts, by lateral movement due to groundwater change (Widdowson, 2007), or by deep weathering of the bedrock. Deep weathering with the formation of iron pans occurs on low-relief surfaces that have been stable for at least a million years (Al-Subbary et al., 1998). Since the Cenozoic, South Africa has been relatively tectonically quiescent (e.g. Bierman et al., 2014). In addition, a favourable climate of high annual rainfall, high humidity and high mean annual temperature is required to form laterites (Widdowson, 2007). Further, higher concentrations of carbon dioxide are also associ-

ated with the formation of laterites (and iron pans). Greenhouse episodes have occurred in the Late Cretaceous and Late Palaeocene to Early Eocene, leading to world-wide extensive weathering (Bardossy, 1981; Valetton, 1983).

Laterite development in southern South Africa is still poorly constrained. It has been argued to be Late Pliocene in age (Marker and Holmes, 1999) and to have continued into the Late Pleistocene (Marker and Holmes, 2005), being a component of the Quaternary development of the Southern Cape (Marker et al., 2002). However, the Mediterranean climate (e.g. more humid) of the coastal areas does not extend inland to the study location, which is expected for laterite development (Brown et al., 1994; Braucher et al., 1998a, b). Given the past climate and tectonic events, the iron pans probably formed during the Late Cretaceous greenhouse episode, which is compounded by the constrained dissection rates of the pediment surfaces (e.g. Dauteuil et al., 2015). The formation of duricrusts and iron pans would have occurred coevally with pediment formation and would have extended post-pediment formation (Helgren and Butzer, 1977; Widdowson, 2007). The presence of iron pans indicates a period of geomorphic stability that could have lasted more than 2 Myr with low (0.3 to 0.6 m Myr⁻¹) denudation rates.

5.4 Sequence of events

Pediment formation requires mountain range retreat, which causes the underlying lithological strata to be truncated (Fig. 15). The *minimum* exposure ages calculated by cosmogenic nuclide dating using the boulder surface samples show remarkably low denudation rates of the pediments during the last 3.8 Myr, which is related to both the lithology (duricrust cappings, resistant quartzite boulders; e.g. Scharf et al., 2013) and the structure of the CFB deflecting incising rivers.

During the Cretaceous the Cape Fold Belt was exhumed (Fig. 15; Tinker et al., 2008a; Tankard et al., 2009). During this time, the folded strata were eroded and planed by hillslope processes (e.g. Rich, 1935; Bourne and Twidale, 1998), depositing colluvial material and then forming soils (Fig. 15) on the alluviated pediments. This was aided by the humid climate and greenhouse conditions of the Cretaceous causing deep weathering (Bardossy, 1981; Valetton, 1983). Tectonic stability allowed the formation of iron pans and duricrusts, which are now exposed at the surface of the alluviated pediments due to surface deflation and the removal of overbank material, as shown by the depth profile (Fig. 15). The initial planation and colluvial build-up had to have occurred pre-Miocene as shown by the dissection data (Tables 4, 5). However, we posit the surfaces could have formed much earlier due to the very slow processes associated with pediment formation (e.g. Lustig, 1969; Dohrenwend and Parsons, 2009). By the mid-Miocene, the dissection of the pediments and backing Cape Fold Belt occurred with the development of small streams and sub-catchments draining the pediments,

with a shift towards a more fluvial-dominated regime. This latter stage of landscape development has decoupled the pediments from the CFB sediment source and essentially fossilised the landform (Table 3), with very low denudation (0.3 to 0.6 m Myr⁻¹) followed by a more recent phase of aeolian deflation.

5.5 Implications for landscape development

The evolution of the pediment surfaces studied in South Africa indicates that the relative importance of hillslope and fluvial processes (including valley development) varies over time. Therefore, the model proposed here does not fit into the previously published model types (Fig. 1) that argued that pediment evolution is dominated by a single process (e.g. “Model 1” in Fig. 1: Gilbert, 1877; Paige, 1912; Howard 1942; “Model 2” in Fig. 1: Lawson, 1915; Rich, 1935; Kesel, 1977; Bourne and Twidale, 1998; Dauteuil et al., 2015) and that the dominant process varies due to lithology (e.g. “Model 3” in Fig. 1: Lustig, 1969; Parsons and Abrahams, 1984) or is assisted by valley/basin development (e.g. “Model 4” in Fig. 1: Lustig, 1969; Parsons and Abrahams, 1984). The change from hillslope to fluvial processes is likely a response to tectonic or climatic perturbations (Fig. 15). The initial formation of the pediments was most likely aided by large-scale erosion during the Cretaceous (e.g. Tinker et al., 2008a, b; Wildman et al., 2015, 2016; Richardson et al., 2017) and tropical climate conditions (Partridge and Maud, 2000).

The indicative geomorphic ages reported here, related to the second phase of development and the dissection of the pediments by small tributaries, roughly correlate to the proposed uplift in the Cenozoic (Green et al., 2016) of 30 Ma (Burke, 1996), 18 Ma (Partridge and Maud, 1987) and 2.5 Ma (Partridge and Maud, 1987) and could indicate that the pediments were dissected due to different pulses of uplift. Nonetheless, this time period also corresponds to variation in climate, including periods of humidity reported to have ended at 30 Ma (Burke, 1996) or 18 Ma (Burke, 1996). It is not possible to distinguish the main driver of dissection, and tectonic signatures are not identified within the Gouritz catchment morphometry (Richardson et al., 2016).

The grading of the pediments implies that the main trunk rivers were active before the development of the pediments, at least by the Miocene and probably within the Cretaceous when large-scale exhumation occurred within South Africa (e.g. Tinker et al., 2008a; Richardson et al., 2017). The individual grading of the pediment surfaces indicates the pediments are relatively local features that react to surrounding tectonic, geological and geomorphological settings and are not singular surfaces (King, 1953). The ¹⁰Be-derived denudation rates of the pediments are some of the lowest in the world (Portenga and Bierman, 2011) and congruent with low geomorphic activity documented by other researchers (Fig. 3 and references therein). There has been a drastic reduction

in denudation rates since the Cretaceous as shown by apatite fission track and cosmogenic nuclide studies (Fig. 3 and references therein). However, surface lowering is not consistent across landforms within southern South Africa. Rivers are dissecting at a faster rate (Scharf et al., 2013; Kounov et al., 2015) than the pediment surfaces (this study; van der Wateren and Dunai, 2001; Bierman et al., 2014; Kounov et al., 2015), which indicates that relief is developing at a slow rate, as also reported by Bierman et al. (2014) from the Eastern Cape. The offshore depositional record (Tinker et al., 2008a) mirrors the reduction in denudation rates, with peaks in the Cenozoic most likely related to the rejuvenation of the landscape, which dissected the pediments in this study (e.g. Hirsch et al., 2010; Dalton et al., 2015; Sonibare et al., 2015). These increases in offshore sediment flux are minor in comparison to rates in the Cretaceous.

6 Conclusion

Large-scale erosional surfaces characterise the ancient landscape of southern South Africa. Denudation rates of the Prince Albert and Laingsburg pediments in the Western Cape are between 0.3 and 1.0 m Myr⁻¹, and the pediments have been exposed before the Early Pleistocene. As most of the pediment surfaces have ¹⁰Be concentrations that approach secular equilibrium, the ¹⁰Be-derived exposure ages provide minimum exposure age estimates. Our study corroborates how CRN depth profiling in alluvial pediments can provide additional information on long-term landscape dynamics and demonstrates how forward modelling can unveil the erosion–exposure age scenarios that most likely explain the observed ¹⁰Be depth concentrations. The existence of a long period of low denudation followed by a recent phase of aeolian deflation merits further study to verify if this is a widespread and characteristic feature of alluviated pediment surfaces in (semi-)arid climatic conditions.

The pediments studied must be at least Miocene in age and probably much older (i.e. Cretaceous) based on the volumes of post-pediment dissection, published erosion rates, the presence of duricrusts and the current understanding of tectonic and climatic variation in the region. The duricrusts represent an internal geomorphic threshold which limits the rate of denudation. The dissection of the pediments has been largely controlled by the structure of the Cape Fold Belt, with the initial geomorphic pulse of incision most likely related to tectonic uplift or climate change. The pediments grade to individual base levels (trunk rivers), and although locally extensive, they are not a regional feature representing one single surface. The presence of the pediments deflected dissecting rivers in some locations and controlled landscape evolution of the surrounding rivers.

The pediments in southern South Africa are lowering at very low rates and are now decoupled from the surrounding rivers. Therefore, they are a fossilised landform that rep-

resents a relatively stable store of sediment in which surface lowering occurs by aeolian erosion causing deflation. The persistence of the pediments is due to the resistant duricrust capping and quartzitic boulders, as well as the structural control of the Cape Fold Belt and pediments, deflecting dissecting rivers. We contend that a multi-proxy approach that combines cosmogenic nuclides with surrounding geomorphologic and stratigraphic conditions provides a more comprehensive picture of long-term landscape dynamics.

Data availability. Cosmogenic data used in this study are provided in the Supplement.

Supplement. The supplement related to this article is available online at <https://doi.org/10.5194/esurf-13-315-2025-supplement>.

Author contributions. JCR, DMH and AL collected the data. Processing and analysis of the data were completed by JCR and VV. Forward modelling work was completed by VV. MC measured the ¹⁰Be / ⁹Be using an accelerator mass spectrometer at the 500 kV Tandy facility at ETH Zürich. VV provided further support processing the data with regards to the depth profile, creating Fig. 9 and writing the methodology for cosmogenic nuclides. JCR led the writing and drafting of figures, with contributions to the text and figures by VV, DMH and AL.

Competing interests. At least one of the (co-)authors is a member of the editorial board of *Earth Surface Dynamics*. The peer-review process was guided by an independent editor, and the authors also have no other competing interests to declare.

Disclaimer. Publisher's note: Copernicus Publications remains neutral with regard to jurisdictional claims made in the text, published maps, institutional affiliations, or any other geographical representation in this paper. While Copernicus Publications makes every effort to include appropriate place names, the final responsibility lies with the authors.

Acknowledgements. Jérôme Schoonejans and Marco Bravin are thanked for their help during laboratory work undertaken at the Université catholique de Louvain, Belgium. David Lee is thanked for his help in improving Fig. 1. The landowners in South Africa are thanked for their permission to enter their land and take samples. The Council for Geoscience is thanked for providing geology GIS tiles under the academic/research license. Alexandre Kounov and Regis Braucher are thanked for their reviews of this paper.

Financial support. This research has been supported by the British Society for Geomorphology (postgraduate award) and the British Sedimentological Research Group (postgraduate award).

Review statement. This paper was edited by Daniella Rempe and reviewed by Regis Braucher and Alexandre Kounov.

References

- Abdelkareem, M., Ghoneim, E., El-Baz, F., and Askalany, M.: New insight on paleoriver development in the Nile basin of the eastern Sahara, *J. Afr. Ear. Sci.*, 62, 35–40, <https://doi.org/10.1016/j.jafrearsci.2011.09.001>, 2012.
- Aguilar, G., Riquelme, R., Martinod, J., Darrozes, J., and Maire, E.: Variability in erosion rates related to the state of landscape transience in the semi-arid Chilean Andes, *Earth Surf. Proc. Land.*, 36, 1736–1748, <https://doi.org/10.1002/esp.2194>, 2011.
- Al-Subbary, A. K., Nichols, G. J., Bosence, D. W. J., and Al-Kadasi, M.: Pre-rift doming, peneplanation or subsidence in the southern Red Sea? Evidence from the Medj-Zir Formation (Tawilah Group) of western Yemen, in: *Sedimentation and Tectonics in Rift Basins Red Sea-Gulf of Aden*, edited by: Purser, B. H. and Bosence, D., Springer Netherlands, 119–134, <https://doi.org/10.1007/978-94-011-4930-3>, 1998.
- Bardossy, G.: Paleoenvironments of laterites and lateritic bauxites – effect of global tectonism on bauxite formation, in: *International Seminar on Lateritisation Processes (Trivandrum, India)*, Balkema, Rotterdam, the Netherlands, 284–297, ISBN 9061912024, 1981.
- Bellin, N., Vanacker, V., and Kubik, P. W.: Denudation rates and tectonic geomorphology of the Spanish Betic Cordillera, *Earth Planet. Sc. Lett.*, 390, 19–30, <https://doi.org/10.1016/j.epsl.2013.12.045>, 2014.
- Bessin, P., Guillocheau, F., Robin, C., Schrötter, J. M., and Bauer, H.: Planation surfaces of the Armorican Massif (western France): Denudation chronology of a Mesozoic land surface twice exhumed in response to relative crustal movements between Iberia and Eurasia, *Geomorph.*, 233, 75–91, <https://doi.org/10.1016/j.geomorph.2014.09.026>, 2015.
- Bierman, P. R. and Caffee, M.: Slow rates of rock surface erosion and sediment production across the Namib Desert and escarpment, southern Africa, *Am. J. Sci.*, 301, 326–358, 2001.
- Bierman, P. R., Coppersmith, R., Hanson, K., Neveling, J., Portenga, E. W., and Rood, D. H.: A cosmogenic view of erosion, relief generation, and the age of faulting in southern Africa, *GSA Today*, 24, 4–11, <https://doi.org/10.1130/GSATG206A.1>, 2014.
- Binnie, A., Binnie, S. A., Parteli, E. J. R., and Dunai, T. J.: The implications of sampling approach and geomorphological processes for cosmogenic ^{10}Be exposure dating of marine terraces, *Nucl. Instrum. Meth. Phys. Res. B*, 467, 130–139, <https://doi.org/10.1016/j.nimb.2019.12.017>, 2020.
- Bishop, P.: Long-term landscape evolution: linking tectonics and surface processes, *Earth Surf. Proc. Land.*, 32, 329–365, <https://doi.org/10.1002/esp.1493>, 2007.
- Bloom, A. L.: Teaching about relict, no-analog landscapes, *Geomorph.*, 47, 303–311, [https://doi.org/10.1016/S0169-555X\(02\)00094-6](https://doi.org/10.1016/S0169-555X(02)00094-6), 2002.
- Bourne, J. A. and Twidale, C. R.: Pediments and alluvial fans: genesis and relationships in the western piedmont of the Flinders Ranges, South Australia, *Aust. J. Earth Sci.*, 45, 123–135, <https://doi.org/10.1080/08120099808728373>, 1998.
- Braucher, R., Bourles, D. L., Colin, F., Brown, E. T., and Boulange, B.: Brazilian laterite dynamics using in situ-produced ^{10}Be , *Earth Planet. Sc. Lett.*, 163, 197–205, [https://doi.org/10.1016/S0012-821X\(98\)00187-3](https://doi.org/10.1016/S0012-821X(98)00187-3), 1998a.
- Braucher, R., Colin, F., Brown, E. T., Bourles, D. L., Bamba, O., Raisbeck, G. M., You, F., and Koud, J. M.: African laterite dynamics using in situ-produced ^{10}Be , *Geochem. Cosmo. Acta*, 62, 1501–1507, [https://doi.org/10.1016/S0016-7037\(98\)00085-4](https://doi.org/10.1016/S0016-7037(98)00085-4), 1998b.
- Braucher, R., Merchel, S., Borgomano, J., and Bourlès, D. L.: Production of cosmogenic radionuclides at great depth: A multielement approach, *Earth Planet. Sc. Lett.*, 309, 1–9, <https://doi.org/10.1016/j.epsl.2011.06.036>, 2011.
- Braun, J., Guillocheau, F., Robin, C., Baby, G., and Jelsma, H.: Rapid erosion of the Southern African Plateau as it climbs over a mantle superswell, *J. Geophys. Res.-Sol. Ea.*, 119, 6093–6112, <https://doi.org/10.1002/2014JB010998>, 2014.
- Brocklehurst, S. H. and Whipple, K. X.: Glacial erosion and relief production in the Eastern Sierra Nevada, California, *Geomorph.*, 42, 1–24, [https://doi.org/10.1016/S0169-555X\(01\)00069-1](https://doi.org/10.1016/S0169-555X(01)00069-1), 2002.
- Brook, E. J., Brown, E. T., Kurz, M. D., Ackert, R. P., Raisbeck, G. M., and Yiou, F.: Constraints on age, erosion, and uplift of Neogene glacial deposits in the Transantarctic Mountains determined from in situ cosmogenic ^{10}Be and ^{26}Al , *Geol.*, 23, 1063–1066, [https://doi.org/10.1130/0091-7613\(1995\)023<1063:COAEAU>2.3.CO;2](https://doi.org/10.1130/0091-7613(1995)023<1063:COAEAU>2.3.CO;2), 1995.
- Brown, E. T., Bourlès, D. L., Colin, F., Sanfo, Z., Raisbeck, G. M., and Yiou, F.: The development of iron crust lateritic systems in Burkina Faso, West Africa examined with in-situ-produced cosmogenic nuclides, *Earth Planet. Sc. Lett.*, 124, 19–33, [https://doi.org/10.1016/0012-821X\(94\)00087-5](https://doi.org/10.1016/0012-821X(94)00087-5), 1994.
- Brown, R. W., Rust, D. J., Summerfield, M. A., Gleadow, A. J., and De Wit, M. C.: An Early Cretaceous phase of accelerated erosion on the south-western margin of Africa: Evidence from apatite fission track analysis and the offshore sedimentary record, *Int. J. Rad. Appl. Instr. A. Part D. Nucl. Tracks Radiat. Meas.*, 17, 339–350, [https://doi.org/10.1016/1359-0189\(90\)90056-4](https://doi.org/10.1016/1359-0189(90)90056-4), 1990.
- Brown, R. W., Summerfield, M. A., and Gleadow, A. J. W.: Denudation history along a transect across the Drakensberg Escarpment of southern Africa derived from apatite fission track thermochronology, *J. Geophys. Res.*, 107, 1–18, <https://doi.org/10.1029/2001JB000744>, 2002.
- Bryan, K.: Erosion and sedimentation in the Papago country, Arizona, *U.S. Geol. Surv. Bull.*, 730, 19–90, 1923.
- Burbank, D. W., Leland, J., Fielding, E., Anderson, R. S., Brozovic, N., Reid, M. R., and Duncan, C.: Bedrock incision, rock uplift and threshold hillslopes in the northwestern Himalayas, *Nature*, 379, 505–510, 1996.
- Burke, K.: The African plate, *S. Afri. J. Geol.*, 99, 341–409, 1996.
- Carignano, C., Cioccale, M., and Rabassa, J.: Landscape antiquity of the Central Eastern Sierras Pampeanas (Argentina): Geomorphological evolution since Gondwanic times, *Z. Geomorph. Supplement Band*, 118, 245–268, 1999.
- Chadwick, O. A., Roering, J. J., Heimsath, A. M., Levick, S. R., Asner, G. P., and Khomo, L.: Shaping post-orogenic landscapes by climate and chemical weathering, *Geol.*, 41, 1171–1174, <https://doi.org/10.1130/G34721.1>, 2013.
- Chappell, J., Zheng, H., and Fifield, K.: Yangtze River sediments and erosion rates from source to sink traced with cosmogenic ^{10}Be

- Be: Sediments from major rivers, *Palaeo. Palaeo. Palaeo.*, 241, 79–94, <https://doi.org/10.1016/j.palaeo.2006.06.010>, 2006.
- Chmeleff, J., von Blanckenburg, F., Kossert, K., and Jakob, D.: Determination of the ^{10}Be half-life by multicollector ICP-MS and liquid scintillation counting, *Nucl. Instrum. Meth. Phys. Res. B*, 263, 192–199, <https://doi.org/10.1016/j.nimb.2009.09.012>, 2010.
- Chorley, R. J., Schumm, S. A., and Sugden, D. E.: *Geomorphology*, Methuen and Co., London, 648 pp., <https://doi.org/10.4324/9780429273636>, 1984.
- Christl, M., Vockenhuber, C., Kubik, P. W., Wacker, L., Lachner, J., Alfimov, V., and Sinal, H.-A.: The ETH Zurich AMS facilities: Performance parameters and reference materials, *Nucl. Instrum. Meth. Phys. Res. B*, 294, 29–38, <https://doi.org/10.1016/j.nimb.2012.03.004>, 2–13, 2013.
- Cockburn, H. A. P., Brown, R. W., Summerfield, M. A., and Seidl, M. A.: Quantifying passive margin denudation and landscape development using a combined fission-track thermochronology and cosmogenic isotope analysis approach, *Earth Planet. Sc. Lett.*, 179, 429–435, [https://doi.org/10.1016/S0012-821X\(00\)00144-8](https://doi.org/10.1016/S0012-821X(00)00144-8), 2000.
- Codilean, A. T., Bishop, P., Stuart, F. M., Hoey, T. B., Fabel, D., and Freeman, S. P.: Single-grain cosmogenic ^{21}Ne concentrations in fluvial sediments reveal spatially variable erosion rates, *Geol.*, 36, 159–162, <https://doi.org/10.1130/G24360A.1>, 2008.
- Dalton, T. J. S., Paton, D. A., Needham, T., and Hodgson, N.: Temporal and spatial evolution of deepwater fold thrust belts: Implications for quantifying strain imbalance, *Interpret.*, 3, SAA59–SAA70, <https://doi.org/10.1190/INT-2015-0034.1>, 2015.
- Darvill, C. M., Bentley, M. J., Stokes, C. R., Hein, A. S., and Rodés, Á.: Extensive MIS 3 glaciation in southernmost Patagonia revealed by cosmogenic nuclide dating of outwash sediments, *Earth Planet. Sc. Lett.*, 429, 157–169, <https://doi.org/10.1016/j.epsl.2015.07.030>, 2015.
- Dauteuil, O., Bessin, P., and Guillocheau, F.: Topographic growth around the Orange River valley, southern Africa: A Cenozoic record of crustal deformation and climatic change, *Geomorph.*, 233, 5–19, <https://doi.org/10.1016/j.geomorph.2014.11.017>, 2015.
- Davis, W. M.: Observations in South Africa, *Geol. Soc. Am. Bull.*, 17, 377–450, 1906.
- Dean, W. R. J., Hoffinan, M. T., Meadows, M. E., and Milton, S. J.: Desertification in the semi-arid Karoo, South Africa: review and reassessment, *J. Arid Env.*, 30, 247–264, [https://doi.org/10.1016/S0140-1963\(05\)80001-1](https://doi.org/10.1016/S0140-1963(05)80001-1), 1995.
- Decker, J. E., Niedermann, S., and de Wit, M. J.: Soil erosion rates in South Africa compared with cosmogenic ^3He -based rates of soil production, *S. Afri. J. Geol.*, 114, 475–488, <https://doi.org/10.2113/gssajg.114.3-4.475>, 2011.
- Decker, J. E., Niedermann S., and de Wit, M. J.: Climatically influenced denudation rates of the southern African plateau: Clues to solving a geomorphic paradox, *Geomorph.*, 190, 48–60, <https://doi.org/10.1016/j.geomorph.2013.02.007>, 2013.
- Demoulin, A., Zárate, M., and Rabassa, J.: Long-term landscape development: a perspective from the southern Buenos Aires ranges of east central Argentina, *J. S. Am. Earth Sci.*, 19, 193–204, <https://doi.org/10.1016/j.jsames.2004.12.001>, 2005.
- De Smith, M. J., Goodchild, M. F., and Longley, P.: *Geospatial analysis: a comprehensive guide to principles, techniques and software tools*, Troubador Publishing Ltd., p. 389, ISBN 1905886608, 2007.
- de Wit, M.: The Kalahari Epeirogeny and climate change: differentiating cause and effect from core to space, *S. Afri. J. Geol.*, 110, 367–392, <https://doi.org/10.2113/gssajg.110.2-3.367>, 2007.
- Dirks, P. H., Kibii, J. M., Kuhn, B. F., Steininger, C., Churchill, S. E., Kramers, J. D., Pickering, R., Farber, D. L., Mériaux, A. S., Herries, A. I., and King G. C.: Geological setting and age of Australopithecus sediba from southern Africa, *Science*, 328, 205–208, <https://doi.org/10.1126/science.1184950>, 2010.
- Dixey, F.: African landscape, *Geograph. Rev.*, 34, 457–465, <https://doi.org/10.2307/209976>, 1944.
- Dohrenwend, J. C. and Parsons, A. J.: Pediments in arid environments, in: *Geomorphology of desert environments*, edited by: Abrahams, A. D. and Parsons, A. J., Springer Netherlands, 377–411, <https://doi.org/10.1007/978-1-4020-5719-9>, 2009.
- Doucouré, C. M. and de Wit, M. J.: Old inherited origin for the present near bimodal topography of Africa, *J. Afri. Earth Sci.*, 36, 371–388, [https://doi.org/10.1016/S0899-5362\(03\)00019-8](https://doi.org/10.1016/S0899-5362(03)00019-8), 2003.
- Dunai, T. J.: Scaling factors for production rates of in situ produced cosmogenic nuclides: a critical reevaluation, *Earth Planet. Sc. Lett.*, 176, 157–169, [https://doi.org/10.1016/S0012-821X\(99\)00310-6](https://doi.org/10.1016/S0012-821X(99)00310-6), 2000.
- Dunai, T. J.: *Cosmogenic Nuclides: Principles, Concepts and Applications in the Earth Surface Sciences*, Cambridge University Press, Cambridge, UK, <https://doi.org/10.1017/CBO9780511804519>, 2010.
- Dunai, T. J., López, G. A. G., and Juez-Larré, J.: Oligocene–Miocene age of aridity in the Atacama Desert revealed by exposure dating of erosion-sensitive landforms, *Geol.*, 33, 321–324, <https://doi.org/10.1130/G21184.1>, 2005.
- Du Toit, A.: *Our Wandering Continents: An hypothesis of Continental Drifting*, Oliver and Boyd, UK, 366 pp., ISBN 0598627588, 1937.
- Du Toit, A.: *The Geology of South Africa*, 3rd edn., Oliver and Boyd, UK, 539 pp., 1954.
- Ebinger, C. J. and Sleep, N. H.: Cenozoic magmatism throughout east Africa resulting from impact of a single plume, *Nature*, 395, 788–791, 1998.
- Erlanger, E. D., Granger, D. E., and Gibbon, R. J.: Rock uplift rates in South Africa from isochron burial dating of fluvial and marine terraces, *Geol.*, 40, 1019–1022, <https://doi.org/10.1130/G33172.1>, 2012.
- Fleming, A., Summerfield, M. A., Stone, J. O., Fifield, L. K., and Cresswell, R. G.: Denudation rates for the southern Drakensberg escarpment, SE Africa, derived from in-situ-produced cosmogenic ^{36}Cl : initial results, *J. Geol. Soc.*, 156, 209–212, <https://doi.org/10.1144/gsjgs.156.2.0209>, 1999.
- Flowers, R. M. and Schoene, B.: (U-Th)/He thermochronometry constraints on unroofing of the eastern Kaapvaal craton and significance for uplift of the southern African Plateau, *Geol.*, 38, 827–830, <https://doi.org/10.1130/G30980.1>, 2010.
- Frimmel, H. E., Fölling, P. G., and Diamond, R.: Metamorphism of the Permo-Triassic Cape Fold Belt and its basement, South Africa, *Min. Pet.*, 73, 325–346, 2001.
- Gallagher, K. and Brown, R.: The Mesozoic denudation history of the Atlantic margins of southern Africa and southeast Brazil and the relationship to offshore sedi-

- mentation, *Geol. Soc., London, Sp. Pub.*, 153, 41–53, <https://doi.org/10.1144/GSL.SP.1999.153.01.03>, 1999.
- Ghosh, P., Sinha, S., and Misra, A.: Morphometric properties of the trans-Himalayan river catchments: Clues towards a relative chronology of orogen-wide drainage integration, *Geomorph.*, 233, 127–141, <https://doi.org/10.1016/j.geomorph.2014.10.035>, 2014.
- Gilbert, G. K.: Report on the geology of the Henry Mountains. US Geographical and Geological Survey of the Rocky Mountain Region, U.S. Department of the Interior, Washington, DC, <https://doi.org/10.3133/70039916>, 1877.
- Gorelov, S. K., Drenev, N. V., Meschcheryakov, Y. A., Tikanov, N. A., and Fridland, V. M.: Planation surfaces of the USSR, *Geomorph.*, 1, 18–29, 1970.
- Granger, D. E., Kirchner, J. W., and Finkel, R. C.: Quaternary downcutting rate of the New River, Virginia, measured from differential decay of cosmogenic ^{26}Al and ^{10}Be in cave-deposited alluvium, *Geol.*, 25, 107–110, [https://doi.org/10.1130/0091-7613\(1997\)025<0107:QDROTN>2.3.CO;2](https://doi.org/10.1130/0091-7613(1997)025<0107:QDROTN>2.3.CO;2), 1997.
- Green, P. F., Duddy, I. R., Japsen P., Bonow, J. M., and Malan, J. A.: Post-breakup burial and exhumation of the southern margin of Africa, *Basin Res.*, 29, 96–127, <https://doi.org/10.1111/bre.12167>, 2016.
- Guillocheau, F., Chelalou, R., Linol, B., Dauteuil, O., Robin, C., Mvondo, F., Callec, Y., and Colin, J. P.: Cenozoic landscape evolution in and around the Congo Basin: constraints from sediments and planation surfaces, in: *Geology and Resource Potential of the Congo Basin*, edited by: de Wit, M. J., Guillocheau, F., and de Wit, M. C. J., *Regional Geology Reviews*, Springer, 271–313, <https://doi.org/10.1007/978-3-642-29482-2>, 2015.
- Guillocheau, F., Simon, B., Baby, G., Bessin, P., Robin, C., and Dauteuil, O.: Planation surfaces as a record of mantle dynamics: the case example of Africa, *Gondwana Res.*, 53, 82–98, <https://doi.org/10.1016/j.gr.2017.05.015>, 2018.
- Gunnell, Y., Braucher, R., Bourles, D., and André, G.: Quantitative and qualitative insights into bedrock landform erosion on the South Indian craton using cosmogenic nuclides and apatite fission tracks, *Geol. Soc. Am. Bull.*, 119, 576–585, <https://doi.org/10.1130/B25945.1>, 2007.
- Hagedorn, J.: Silcretes in the Western Little Karoo and their relation to geomorphology and palaeoecology, *Palaeoecol. Afr.*, 19, 371–375, 1988.
- Hansma, J., Tohver, E., Schrank, C., Jourdan, F., and Adams, D.: The timing of the Cape Orogeny: New $^{40}\text{Ar}/^{39}\text{Ar}$ age constraints on deformation and cooling of the Cape Fold Belt, South Africa, *Gondwana Res.*, 32, 122–137, <https://doi.org/10.1016/j.gr.2015.02.005>, 2016.
- Helgren, D. M. and Butzer, K. W.: Paleosols of the southern Cape Coast, South Africa: implications for laterite definition, genesis, and age, *Geograph. Rev.*, 67, 430–445, <https://doi.org/10.2307/213626>, 1977.
- Hein, A. S., Hulton, N. R., Dunai, T. J., Schnabel, C., Kaplan, M. R., Naylor, M., and Xu, S.: Middle Pleistocene glaciation in Patagonia dated by cosmogenic-nuclide measurements on outwash gravels, *Earth Planet. Sc. Lett.*, 286, 184–197, <https://doi.org/10.1016/j.epsl.2009.06.026>, 2009.
- Hirsch, K. K., Scheck-Wenderoth, M., van Wees, J. D., Kuhlmann, G., and Paton, D. A.: Tectonic subsidence history and thermal evolution of the Orange Basin, *Mar. Petrol. Geol.*, 27, 565–584, <https://doi.org/10.1016/j.marpetgeo.2009.06.009>, 2010.
- Howard, A. D.: Pediment passes and the pediment problem, *Journal of Geomorphology*, 5, 3–31, 95–136, 1942.
- Jackson J., Ritz, J. F., Siame, L., Raisbeck, G., Yiou, F., Norris, R., Youngson, J., and Bennett, E.: Fault growth and landscape development rates in Otago, New Zealand, using in situ cosmogenic ^{10}Be , *Earth Planet. Sc. Lett.*, 195, 185–193, [https://doi.org/10.1016/S0012-821X\(01\)00583-0](https://doi.org/10.1016/S0012-821X(01)00583-0), 2002.
- Jerolmack, D. J. and Paola, C.: Shredding of environmental signals by sediment transport, *Geophys. Res. Lett.*, 37, L19401, <https://doi.org/10.1029/2010GL044638>, 2010.
- Johnson, M. R., Van Vuuren, C. J., Hegenberger, W. F., Key, R., and Show, U.: Stratigraphy of the Karoo Supergroup in southern Africa: an overview, *J. African Earth Sci.*, 23, 3–15, [https://doi.org/10.1016/S0899-5362\(96\)00048-6](https://doi.org/10.1016/S0899-5362(96)00048-6), 1995.
- Keen-Zebert, A., Tooth, S., and Stuart, F. M.: Cosmogenic ^3He measurements provide insight into lithologic controls on bedrock channel incision: examples from the South African interior, *J. Geol.*, 124, 423–434, <https://doi.org/10.1086/685506>, 2016.
- Kesel, R. H.: Some aspects of the geomorphology of inselbergs in central Arizona, USA, *Z. Geomorph.*, 21, 119–146, 1977.
- King, L. C.: On the ages of African land-surfaces, *Quart. J. Geol. Soc.*, 104, 439–445, <https://doi.org/10.1144/GSL.JGS.1948.104.01-04.20>, 1948.
- King, L. C.: The pediment landform: some current problems, *Geol. Mag.*, 86, 245–250, <https://doi.org/10.1017/S0016756800074665>, 1949.
- King, L. C.: The geology of the Makapan and other caves, *Trans. Royal Soc. S. Afr.*, 33, 121–151, <https://doi.org/10.1080/00359195109519881>, 1951.
- King, L. C.: Canons of landscape evolution, *Geol. Soc. Am. Bull.*, 64, 721–752, [https://doi.org/10.1130/0016-7606\(1953\)64\[721:COLE\]2.0.CO;2](https://doi.org/10.1130/0016-7606(1953)64[721:COLE]2.0.CO;2), 1953.
- King, L. C.: Pediplanation and isostasy: an example from South Africa, *Quart. J. Geol. Soc.*, 111, 353–359, <https://doi.org/10.1144/GSL.JGS.1955.111.01-04.18>, 1955.
- King, L. C.: A geomorphological comparison between Eastern Brazil and Africa (Central and Southern), *Quart. J. Geol. Soc.*, 112, 445–474, <https://doi.org/10.1144/GSL.JGS.1956.112.01-04.22>, 1956a.
- King, L. C.: A geomorfologia do Brasil oriental, *Rev. Bras. Geog.*, 18, 186–263, 1956b.
- King, L. C.: South African scenery. A textbook of geomorphology, Hafner Publishing Co, 308 pp., ISBN 1114475181, 1963.
- Kounov, A., Niedermann, S., de Wit, M. J., Viola, G., Andreoli, M., and Erzinger, J.: Present denudation rates at selected sections of the South African escarpment and the elevated continental interior based on cosmogenic ^3He and ^{21}Ne , *S. Afri. J. Geol.*, 110, 235–248, <https://doi.org/10.2113/gssajg.110.2-3.235>, 2007.
- Kounov, A., Viola, G., De Wit, M., and Andreoli, M. A. G.: Denudation along the Atlantic passive margin: new insights from apatite fission-track analysis on the western coast of South Africa. *Geol. Soc., London, Sp. Pub.*, 324, 287–306, <https://doi.org/10.1144/SP324.19>, 2009.
- Kounov, A., Niedermann, S., de Wit, M. J., Codilean, A. T., Viola, G., Andreoli, M., and Christl, M.: Cosmogenic ^{21}Ne and ^{10}Be reveal a more than 2 Ma Alluvial Fan Flanking the

- Cape Mountains, South Africa, *S. Afr. J. Geol.*, 118, 129–144, <https://doi.org/10.2113/gssajg.118.2.129>, 2015.
- Kubik, P. W. and Christl, M.: ¹⁰Be and ²⁶Al measurements at the Zurich 6 MV Tandem AMS facility, *Nucl. Instrum. Meth. Phys. Res. B*, 268, 880–883, <https://doi.org/10.1016/j.nimb.2009.10.054>, 2010.
- Lawson, A. C.: The epigene profiles of the desert, *Uni. California Dept. Geol. Bull.*, 9, 23–48, 1915.
- Lidmar-Bergström, K.: Exhumed cretaceous landforms in south Sweden, *Z. Geomorph., Supp. Band*, 72, 21–40, 1988.
- Lustig, L. K.: Trend surface analysis of the Basin and Range province, and some geomorphic implications, *US Geol. Surv. Profess. Paper* 500-D, <https://doi.org/10.3133/pp500D>, 1969.
- Margerison, H. R., Phillips, W. M., Stuart, F. M., and Sugden, D. E.: Cosmogenic ³He concentrations in ancient flood deposits from the Coombs Hills, northern Dry Valleys, East Antarctica: interpreting exposure ages and erosion rates, *Earth Planet. Sc. Lett.*, 230, 163–175, <https://doi.org/10.1016/j.epsl.2004.11.007>, 2005.
- Marker, M. E. and Holmes, P. J.: Laterisation on limestones of the Tertiary Wankoe Formation and its relationship to the African Surface, southern Cape, South Africa, *Catena*, 38, 1–21, [https://doi.org/10.1016/S0341-8162\(99\)00066-1](https://doi.org/10.1016/S0341-8162(99)00066-1), 1999.
- Marker, M. E. and Holmes, P. J.: Landscape evolution and landscape sensitivity: the case of the southern Cape, *S. Afr. J. Sci.*, 101, 53–60, 2005.
- Marker, M. E., McFarlane, M. J., and Wormald, R. J.: A laterite profile near Albertinia, Southern Cape, South Africa: its significance in the evolution of the African Surface, *S. Afr. J. Geol.*, 105, 67–74, <https://doi.org/10.2113/1050067>, 2002.
- Midgley, G. F., Hannah, L., Millar, D., Thuiller, W., and Booth, A.: Developing regional and species-level assessments of climate change impacts on biodiversity in the Cape Floristic Region, *Bio. Cons.*, 112, 87–97, [https://doi.org/10.1016/S0006-3207\(02\)00414-7](https://doi.org/10.1016/S0006-3207(02)00414-7), 2003.
- Moore, A., Blenkinsop, T., and Cotterill, F. W.: Southern African topography and erosion history: plumes or plate tectonics?, *Terra Nova*, 21, 310–315, <https://doi.org/10.1111/j.1365-3121.2009.00887.x>, 2009.
- Mountain, E. D.: Grahamstown peneplain, *Trans. Geol. Soc. S Afr.*, 83, 47–53, 1980.
- Norton, K. P. and Vanacker, V.: Effects of terrain smoothing on topographic shielding correction factors for cosmogenic nuclide-derived estimates of basin-averaged denudation rates, *Earth Surf. Proc. Land.*, 34, 145–154, <https://doi.org/10.1002/esp.1700>, 2009.
- Nyblade, A. A. and Robinson, S. W.: The african superswell, *Geophys. Res. Lett.*, 21, 765–768, <https://doi.org/10.1029/94GL00631>, 1994.
- Ollier, C.: *Ancient Landforms*, Belhaven Press, London/New York, 233 pp., ISBN 1-85293-074-6, 1991.
- Ollier, C. and Pain, C.: *The origin of mountains*. Routledge, London/New York, 345 pp., ISBN 9780415198905, 2000.
- Ouimet, W. B., Whipple, K. X., Crosby, B. T., Johnson, J. P., and Schildgen, T. F.: Epigenetic gorges in fluvial landscapes, *Earth Surf. Proc. Land.*, 33, 1993–2009, <https://doi.org/10.1002/esp.1650>, 2008.
- Owen, L. A., Finkel, R. C., Barnard, P. L., Haizhou, M., Asahi, K., Caffee, M. W., and Derbyshire, E.: Climatic and topographic controls on the style and timing of Late Quaternary glaciation throughout Tibet and the Himalaya defined by ¹⁰Be cosmogenic radionuclide surface exposure dating, *Quaternary Sci. Rev.*, 24, 1391–1411, <https://doi.org/10.1016/j.quascirev.2004.10.014>, 2005.
- Paige, S.: Rock-cut surfaces in the desert regions, *J. Geol.*, 20, 442–50, 1912.
- Panario, D., Gutiérrez, O., Sánchez Bettucci, L., Peel, E., Oyhançabal, P., and Rabassa, J.: Ancient landscapes of Uruguay, in: *Gondwana landscapes in southern South America*, edited by: Rabassa, J. and Ollier, C., Springer Dordrecht, 161–199, <https://doi.org/10.1007/978-94-007-7702-6>, 2014.
- Parsons, A. J. and Abrahams, A. D.: Mountain mass denudation and piedmont formation in the Mojave and Sonoran Deserts, *Am. J. Sci.*, 284, 255–271, 1984.
- Partridge, T. C.: Cainozoic environmental change in southern Africa, with special emphasis on the last 200 000 years, *Prog. Phys. Geog.*, 21, 3–22, <https://doi.org/10.1177/030913339702100102>, 1997.
- Partridge, T. C.: Of diamonds, dinosaurs and diastrophism: 150 million years of landscape evolution in southern Africa, *S. Afr. J. Geol.*, 101, 165–184, 1998.
- Partridge, T. C.: *Evolution of Landscapes*, in: *Vegetation of southern Africa*, edited by: Cowling, R. M., Richardson, D. M., and Pierce, S. M., Cambridge University Press, 1–20, ISBN 0521571421, 1999.
- Partridge, T. C. and Maud, R. R.: Geomorphic evolution of southern Africa since the Mesozoic, *S. Afr. J. Geol.*, 90, 179–208, 1987.
- Partridge, T. C. and Maud, R. R. (Eds.): *Macro-scale geomorphic evolution of southern Africa, The Cenozoic of southern Africa*, Oxford University Press, 3–18, ISBN 9780195125306, 2000.
- Paton, D. A.: Influence of crustal heterogeneity on normal fault dimensions and evolution: southern South Africa extensional system, *J. Struct. Geol.*, 28, 868–886, <https://doi.org/10.1016/j.jsg.2006.01.006>, 2006.
- Peulvast, J. P. and Bétard F.: A history of basin inversion, scarp retreat and shallow denudation: The Araripe basin as a keystone for understanding long-term landscape evolution in NE Brazil, *Geomorph.*, 233, 20–40, <https://doi.org/10.1016/j.geomorph.2014.10.009>, 2015.
- Portenga, E. W. and Bierman, P. R.: Understanding Earth's eroding surface with ¹⁰Be, *GSA Today*, 21, 4–10, <https://doi.org/10.1130/G111A.1>, 2011.
- Rich, J. L.: Origin and evolution of rock fans and pediments, *Bull. Geol. Soc. Am.*, 46, 999–1024, <https://doi.org/10.1130/GSAB-46-999>, 2935, 1935.
- Richardson, J. C., Hodgson, D. M., Wilson, A., Carrivick, J. L., and Lang, A.: Testing the applicability of morphometric characterisation in discordant catchments to ancient landscapes: A case study from southern Africa, *Geomorph.*, 201, 162–176, <https://doi.org/10.1016/j.geomorph.2016.02.026>, 2016.
- Richardson, J. C., Hodgson, D. M., Paton, D., Craven, B., Rawcliffe, A., and Lang, A.: Where is my sink? Reconstruction of landscape development in southwestern Africa since the Late Jurassic, *Gondwana Res.*, 45, 43–64, <https://doi.org/10.1016/j.gr.2017.01.004>, 2017.
- Rogers, C. A.: The geological history of the Gouritz River system, *Trans. S. Afri. Phil. Soc.*, 14, 375–384, 1903.
- Romans, B. W., Castelltort, S., Covault, J. A., Fildani, A., and Walsh, J. P.: Environmental signal propagation in sedimen-

- tary systems across timescales, *Earth-Sci. Rev.*, 153, 7–29, <https://doi.org/10.1016/j.earscirev.2015.07.012>, 2016.
- Ruszkiczay-Rüdiger, Z., Braucher, R., Csillag, G., Fodor, L. I., Dunai, T. J., Bada, G., Bourlés, D., and Müller, P.: Dating Pleistocene aeolian landforms in Hungary, Central Europe, using in situ produced cosmogenic ^{10}Be , *Quat. Geochron.*, 6, 515–529, <https://doi.org/10.1016/j.quageo.2011.06.001>, 2011.
- Scharf, T. E., Codilean, A. T., de Wit, M., Jansen, J. D., and Kubik, P. W.: Strong rocks sustain ancient postorogenic topography in southern Africa, *Geol.*, 41, 331–334, <https://doi.org/10.1130/G33806.1>, 2013.
- Sharp, R. P.: Geomorphology of the Ruby–East Humboldt Range, Nevada, *Bull. Geol. Soc. Am.*, 51, 337–372, <https://doi.org/10.1130/GSAB-51-337>, 1940.
- Sømme, T. O., Piper, D. J., Deptuck, M. E., and Helland-Hansen, W.: Linking onshore–offshore sediment dispersal in the Golo source-to-sink system (Corsica, France) during the Late Quaternary, *J. Sed. Res.*, 81, 118–137, <https://doi.org/10.2110/jsr.2011.11>, 2011.
- Sonibare, W. A., Sippel, J., Scheck-Wenderoth, M., and Mikeš, D.: Crust-scale 3D model of the Western Bredasdorp Basin (Southern South Africa): data-based insights from combined isostatic and 3D gravity modelling, *Basin Res.*, 27, 125–151, <https://doi.org/10.1111/bre.12064>, 2015.
- Spikings, A. L., Hodgson, D. M., Paton, D. A., and Sychala, Y. T.: Palimpsestic restoration of an exhumed deep-water system: a workflow to improve paleogeographic reconstructions, *Interpretation*, 3, SAA71–SAA87, <https://doi.org/10.1190/INT-2015-0015.1>, 2015.
- Stanley, J. R., Braun, J., Baby, G., Guillocheau, F., Robin, C., Flowers, R. M., Brown, R., Wildman, M., and Beucher, R.: Constraining plateau uplift in southern Africa by combining thermochronology, sediment flux, topography, and landscape evolution modeling, *J. Geophys. Res.-Sol. Ea.*, 126, e2020JB021243, <https://doi.org/10.1029/2020JB021243>, 2021.
- Summerfield, M. A.: Silcrete as a palaeoclimatic indicator: evidence from southern Africa, *Palaeo. Palaeo. Palaeo.*, 41, 65–79, [https://doi.org/10.1016/0031-0182\(83\)90076-7](https://doi.org/10.1016/0031-0182(83)90076-7), 1983.
- Tankard, A., Welsink, H., Aukes, P., Newton, R., and Stettler, E.: Tectonic evolution of the Cape and Karoo basins of South Africa, *Mar. Pet. Geol.*, 26, 1379–1412, <https://doi.org/10.1016/j.marpetgeo.2009.01.022>, 2009.
- Tinker, J., De Wit, M., and Brown, R.: Mesozoic exhumation of the southern Cape, South Africa, quantified using apatite fission track thermochronology, *Tectonophysics*, 455, 77–93, <https://doi.org/10.1016/j.tecto.2007.10.009>, 2008a.
- Tinker, J., de Wit, M., and Brown, R.: Linking source and sink: evaluating the balance between onshore erosion and offshore sediment accumulation since Gondwana break-up, South Africa, *Tectonophysics*, 455, 94–103, <https://doi.org/10.1016/j.tecto.2007.11.040>, 2008b.
- Twidale, C. R.: *Ancient Australian Landscapes*, Rosenberg Pub Pty Limited, 144 pp., ISBN 9781877058448, 2007a.
- Twidale, C. R.: Bornhardts and associated fracture patterns, *Rev. As. Geol. Arg.*, 62, 139–153, 2007b.
- Valeton, I.: Palaeoenvironment of lateritic bauxites with vertical and lateral differentiation, *Geol. Soc., London, Sp. Pub.*, 11, 77–90, <https://doi.org/10.1144/GSL.SP.1983.011.01.10>, 1983.
- Vanacker V., von Blanckenburg, F., Hewawasam, T., and Kubik, P. W.: Constraining landscape development of the Sri Lankan escarpment with cosmogenic nuclides in river sediment, *Earth Planet. Sc. Lett.*, 253, 402–414, <https://doi.org/10.1016/j.epsl.2006.11.003>, 2007.
- Vanacker, V., von Blanckenburg, F., Govers, G., Molina, A., Campforts, B., and Kubik, P. W.: Transient river response, captured by channel steepness and its concavity, *Geomorph.*, 228, 234–243, <https://doi.org/10.1016/j.geomorph.2014.09.013>, 2015.
- van der Beek, P., Summerfield, M. A., Braun, J., Brown, R. W., and Fleming, A.: Modeling postbreakup landscape development and denudational history across the southeast African (Drakensberg Escarpment) margin, *J. Geophys. Res.-Sol. Ea.*, 107, 1–18, <https://doi.org/10.1029/2001JB000744>, 2002.
- Vandermaelen, N., Beerten, K., Clapuyt, F., Christl, M., and Vanacker, V.: Constraining the aggradation mode of Pleistocene river deposits based on cosmogenic radionuclide depth profiling and numerical modelling, *Geochronology*, 4, 713–730, <https://doi.org/10.5194/gchron-4-713-2022>, 2022.
- van der Wateren, F. M. and Dunai, T. J.: Late Neogene passive margin denudation history—cosmogenic isotope measurements from the central Namib desert, *Glob. Planet. Change*, 30, 271–307, [https://doi.org/10.1016/S0921-8181\(01\)00104-7](https://doi.org/10.1016/S0921-8181(01)00104-7), 2001.
- van Niekerk, H. S., Beukes, N. J., and Gutzmer, J.: Post-Gondwana pedogenic ferromanganese deposits, ancient soil profiles, African land surfaces and palaeoclimatic change on the Highveld of South Africa, *J. Afr. Earth Sci.*, 29, 761–781, [https://doi.org/10.1016/S0899-5362\(99\)00128-1](https://doi.org/10.1016/S0899-5362(99)00128-1), 1999.
- Vermesch, P.: CosmoCalc: An Excel add-in for cosmogenic nuclide calculations, *Geochem. Geophys. Geosyst.*, 8, 1–14, <https://doi.org/10.1029/2006GC001530>, 2007.
- von Blanckenburg, F., Belshaw, N., and O’Nions, R.: Separation of ^9Be and cosmogenic ^{10}Be from environmental materials and SIMS isotope dilution analysis, *Chem. Geol.*, 129, 93–99, [https://doi.org/10.1016/0009-2541\(95\)00157-3](https://doi.org/10.1016/0009-2541(95)00157-3), 1996.
- von Blanckenburg, F., Hewawasam, T., and Kubik, P. W.: Cosmogenic nuclide evidence for low weathering and denudation in the wet, tropical highlands of Sri Lanka, *J. Geophys. Res.-Earth*, 109, 1–22, <https://doi.org/10.1029/2003JF000049>, 2004.
- Widdowson, M.: *Laterite and Ferricrete*, in: *Geochemical Sediments and Landscapes*, edited by: Nash, D. J. and McLaren, S. J., Oxford, UK, Wiley-Blackwell, 46–94, ISBN 978-1-405-12519-2, 2007.
- Wildman, M., Brown, R., Watkins, R., Carter, A., Gleadow, A., and Summerfield, M.: Post break-up tectonic inversion across the southwestern cape of South Africa: new insights from apatite and zircon fission track thermochronometry, *Tectonophysics*, 654, 30–55, <https://doi.org/10.1016/j.tecto.2015.04.012>, 2015.
- Wildman, M., Brown, R., Beucher, R., Persano, C., Stuart, F., Gallagher, K., Schwanethal, J., and Carter, A.: The chronology and tectonic style of landscape evolution along the elevated Atlantic continental margin of South Africa resolved by joint apatite fission track and (U-Th-Sm) / He thermochronology, *Tectonics*, 35, 511–545, <https://doi.org/10.1002/2015TC004042>, 2016.
- Wildman, M., Brown, R., Persano, C., Beucher, R., Stuart, F. M., Mackintosh, V., Gallagher, K., Schwanethal, J., and Carter, A.: Contrasting Mesozoic evolution across the boundary between on and off craton regions of the South African plateau inferred from apatite fission track and (U-Th-Sm) / He ther-

- mochronology, *J. Geophys. Res.-Sol. Ea.*, 122, 1517–1547, <https://doi.org/10.1002/2016JB013478>, 2017.
- Willenbring, J. K. and von Blanckenburg, F.: Long-term stability of global erosion rates and weathering during late-Cenozoic cooling, *Nature*, 465, 211–214, 2010.
- Wittmann, H., von Blanckenburg, F., Kruesmann, T., Norton, K. P., and Kubik, P. W.: Relation between rock uplift and denudation from cosmogenic nuclides in river sediment in the Central Alps of Switzerland, *J. Geophys. Res.-Earth*, 112, 1–20, <https://doi.org/10.1029/2006JF000729>, 2007.
- Wittmann, H., Von Blanckenburg, F., Guyot, J. L., Maurice, L., and Kubik, P. W.: From source to sink: Preserving the cosmogenic ^{10}Be -derived denudation rate signal of the Bolivian Andes in sediment of the Beni and Mamoré foreland basins, *Earth Planet. Sc. Lett.*, 288, 463–474, <https://doi.org/10.1016/j.epsl.2009.10.008>, 2009.